

Non-perturbative renormalization of the static axial current in quenched QCD



Jochen Heitger^a, Martin Kurth^b and Rainer Sommer^c

^a Westfälische Wilhelms-Universität Münster, Institut für Theoretische Physik,
Wilhelm-Klemm-Strasse 9, D-48149 Münster, Germany

^b University of Southampton, Department of Physics and Astronomy,
Highfield, Southampton SO17 1BJ, United Kingdom

^c Deutsches Elektronen-Synchrotron DESY, Zeuthen,
Platanenallee 6, D-15738 Zeuthen, Germany

Abstract

We non-perturbatively calculate the scale dependence of the static axial current in the Schrödinger functional scheme by means of a recursive finite-size scaling technique, taking the continuum limit in each step. The bare current in the $O(a)$ improved theory as well as in the original Wilson regularization is thus connected to the renormalization group invariant one. The latter may then be related to the current at the B-scale defined such that its matrix elements differ from the physical (QCD) ones by $O(1/M)$. At present, a (probably small) perturbative uncertainty enters in this step. As an application, we renormalize existing unimproved data on F_B^{bare} and extrapolate to the continuum limit. We also study an interesting function $h(d/L, u)$ derived from the Schrödinger functional amplitude describing the propagation of a static quark-antiquark pair.

Key words: Lattice QCD; Heavy quark effective theory; Static approximation; Non-perturbative renormalization; Schrödinger functional; Renormalization group invariant

PACS: 11.15.Ha; 12.15.Hh; 12.38.Bx; 12.38.Gc; 12.39.Hg; 13.20.He; 14.65.Fy

February 2003

1 Introduction

Since the decay constant F_B , governing the leptonic decay of a B-meson, is an essential element in the quantitative analysis of the unitarity triangle, many lattice QCD investigations have worked towards its determination. However, with its large mass, the b-quark still escapes a direct numerical treatment [1] and effective theories have to be used to separate the large mass scale from the low-energy bound-state dynamics. (As an exception to this rule, it has recently been demonstrated that also finite-volume methods on lattices with a large number of points represent a possible alternative [2, 3].)

The most natural and theoretically appealing effective theory is the *static approximation* [4]. It describes the large-mass limit of the theory and is the starting point for a $1/m$ -expansion, the heavy quark effective theory. Yet the problems of this framework have been twofold in the past. (i) The renormalization properties of the static theory are different, i.e. the renormalization constant Z_A^{stat} of the axial current in $(A_R^{\text{stat}})_0 = Z_A^{\text{stat}}(\mu) \bar{\psi}_d \gamma_0 \gamma_5 \psi_b^{\text{stat}}$ becomes scale (μ) dependent, thereby entailing an additional uncertainty, and (ii) Monte Carlo computations of the matrix element itself are difficult. For these reasons, after a significant initial effort [5, 6, 7, 8, 9, 10, 11, 12], the computation of F_B in the static approximation has received little attention in the recent past.

In the present work, we solve (i) by computing the renormalization factor that relates the bare operator in lattice regularization to the *renormalization group invariant (RGI) operator*. Denoting its matrix element by $\Phi_{\text{RGI}}^{\text{stat}}$, one then has a relation

$$F_B \sqrt{m_B} = C_{\text{PS}}(M_b/\Lambda_{\overline{\text{MS}}}) \times \Phi_{\text{RGI}}^{\text{stat}} + \mathcal{O}(1/M_b) \quad (1.1)$$

with a function C_{PS} of the renormalization group invariant b-quark mass M_b in units of the Λ -parameter. It is scale independent, but in practice it is obtained perturbatively and an uncertainty due to perturbation theory remains, see Section 5. The important task of a lattice computation of the B-meson decay constant in the static approximation is to compute $\Phi_{\text{RGI}}^{\text{stat}}$.

Our strategy to arrive at $\Phi_{\text{RGI}}^{\text{stat}}$ from the bare matrix element follows the one used by the ALPHA Collaboration for the renormalization group invariant quark mass [13]. In this approach, an intermediate finite-volume renormalization scheme is used to follow the scale evolution non-perturbatively to high energies ($\mathcal{O}(100\text{GeV})$), where then perturbation theory can safely be used to connect to the renormalization group invariants. For a more detailed explanation of the overall strategy we refer to Ref. [14] and for a preliminary report on our work to Refs. [15, 16].

The present paper is organized as follows. In Section 2 we discuss our intermediate renormalization scheme, formulated in the Schrödinger functional (SF). It is based on the renormalization condition introduced in [17], but a modification has been necessary to achieve good statistical precision. Section 3 contains the numerical determination of the scale dependence of the current in the SF scheme which is independent of the lattice formulation. We also relate the current renormalized at some proper low scale to the RGI current. Section 4 gives our results for the lattice formulation dependent values of the Z -factor at this low scale. In Section 5 we then discuss Eq. (1.1) and explain in detail how our results are to be used. As an example we obtain $F_{B_s}^{\text{stat}}$ from published numbers of the bare matrix element. We finish with a brief discussion of the results in Section 6. Details of the numerical and perturbative calculations are described in appendices.

2 Intermediate renormalization scheme

In this section we introduce our intermediate renormalization scheme. For reasons to be explained below, it differs from the one originally introduced in Ref. [17]. The perturbative calculations of Ref. [17] are extended to the new scheme in Appendix B.

We choose a mass-independent renormalization scheme, leading to simple renormalization group equations. The scheme is defined using the Schrödinger functional (SF) [18, 19], i.e. the QCD partition function $\mathcal{Z} = \int_{T \times L^3} D[A, \bar{\psi}, \psi] e^{-S[A, \bar{\psi}, \psi]}$ on a $T \times L^3$ cylinder in Euclidean space, where periodic boundary conditions in the spatial directions of length L and Dirichlet boundary conditions at times $x_0 = 0, T$ are imposed on the gluon and quark fields.¹ Their exact form can be found in Ref. [21]. Moreover, we set $T = L$ throughout, and the renormalization scale μ is identified with the inverse box extension, $1/L$. Such a finite-volume renormalization scheme is chosen, since it allows to study the scale dependence in the *continuum limit* for a large range of μ [22, 23, 24, 13]. We can then relate the quantities renormalized at some low scale μ to the RGI quantities. Reviews of the strategy are found in [25, 26, 14], and for a more detailed description the reader should consult Ref. [13] which we will follow quite closely.

As detailed in [17], we consider the SF with vanishing boundary gauge fields and $\theta = 0.5$. These settings are identical to those used for the quark mass renormalization in [13] and were motivated by meeting the criteria of good statistical precision of the Monte Carlo results, well-behaved perturbative expansions of the renormalization group functions and minimization of lattice artifacts [27]. Static quarks are included as discussed in Ref. [17], and we use the notation of that reference. Throughout most of this paper, we formally stay in the framework of continuum QCD; some notation and basic formulae of the lattice regularized theory, in which the following expressions receive a precise meaning, are collected in Appendix A.

In contrast to the relativistic current, there is no axial Ward identity which protects the renormalized static-light axial vector current,

$$(A_{\text{R}}^{\text{stat}})_0(x) = Z_{\text{A}}^{\text{stat}} \bar{\psi}_1(x) \gamma_0 \gamma_5 \psi_{\text{h}}(x), \quad (2.1)$$

from a scale dependence. Its scale evolution is governed by the renormalization group equation

$$\mu \frac{\partial \Phi}{\partial \mu} = \gamma(\bar{g}) \Phi, \quad (2.2)$$

where

$$\Phi \equiv \Phi^{\text{stat}} = \langle f | (A_{\text{R}}^{\text{stat}})_0 | i \rangle \quad (2.3)$$

is an arbitrary matrix element of the renormalized static current. The renormalization group function γ , the anomalous dimension, has a perturbative expansion

$$\gamma(\bar{g}) \stackrel{\bar{g} \rightarrow 0}{\sim} -\bar{g}^2 \left\{ \gamma_0 + \gamma_1 \bar{g}^2 + \gamma_2 \bar{g}^4 + \mathcal{O}(\bar{g}^6) \right\} \quad (2.4)$$

with a universal leading coefficient [28, 29],

$$\gamma_0 = -\frac{1}{4\pi^2}, \quad (2.5)$$

¹The spatial boundary conditions of the quark fields are only periodic up to a global phase θ [20], an additional ‘kinematical’ parameter.

and $\gamma_1, \gamma_2, \dots$ depending on the chosen renormalization scheme.

Non-perturbatively, one computes the change of Φ under finite changes of the renormalization scale. For a scale factor of two, the induced change defines the *step scaling function*,

$$\sigma_A^{\text{stat}}(u) = \Phi(\mu/2)/\Phi(\mu) = Z_A^{\text{stat}}(2L)/Z_A^{\text{stat}}(L), \quad (2.6)$$

whose argument $u \equiv \bar{g}^2(L)$ is taken to be exactly the coupling defined in [24], and as always in the SF we have $\mu = 1/L$.

2.1 The old scheme

In Ref. [17], a normalization condition was formulated in terms of suitable correlation functions defined in the SF. It reads

$$Z_A^{\text{stat}}(L) X(L) = X^{(0)}(L) \quad \text{at vanishing quark mass,} \quad (2.7)$$

with

$$X(L) = \frac{f_A^{\text{stat}}(L/2)}{\sqrt{f_1^{\text{stat}}}} \quad (2.8)$$

and $X^{(0)}(L)$ the tree-level value of $X(L)$. Here, f_A^{stat} is a correlation function between a static-light pseudoscalar boundary source and A_0^{stat} in the bulk, and f_1^{stat} denotes the correlator between two such boundary sources at $x_0 = 0$ and $x_0 = T$:

$$f_A^{\text{stat}}(x_0) = -\frac{1}{2} \int d^3\mathbf{y} d^3\mathbf{z} \langle A_0^{\text{stat}}(x) \bar{\zeta}_h(\mathbf{y}) \gamma_5 \zeta_l(\mathbf{z}) \rangle, \quad (2.9)$$

$$f_1^{\text{stat}} = -\frac{1}{2L^6} \int d^3\mathbf{u} d^3\mathbf{v} d^3\mathbf{y} d^3\mathbf{z} \langle \bar{\zeta}_l'(\mathbf{u}) \gamma_5 \zeta_h'(\mathbf{v}) \bar{\zeta}_h(\mathbf{y}) \gamma_5 \zeta_l(\mathbf{z}) \rangle. \quad (2.10)$$

(For the proper definition of the ‘boundary quark and antiquark fields’ $\zeta, \bar{\zeta}$ we refer to Refs. [17, 21].) The two correlators are schematically depicted in Figure 1, and their explicit form on the lattice is given in Eqs. (A.10) and (A.13) of Appendix A.1. In the ratio (2.8) both



Figure 1: Sketch of the correlation functions $f_A^{\text{stat}}(x_0)$ (left) and f_1^{stat} (right). The single and double lines represent light (i.e. relativistic) and static quark propagators, respectively.

the multiplicative renormalization of the boundary quark fields and the mass counterterm of the static field cancel.

We now have to point out a drawback of this scheme that only becomes evident, when it is implemented numerically. Namely, the lattice step scaling function $\Sigma_A^{\text{stat}}(u, a/L)$ (cf. Eq. (A.20) for its definition), computed by means of Monte Carlo simulations, has large statistical errors at $u \approx 1.5$ and larger. In particular, these errors grow with L/a . This can be inferred from the results tabulated in Appendix A.2 and is illustrated for three representative coupling values in Figure 2. For $L/a = 12, 16$ (which amounts to also calculate

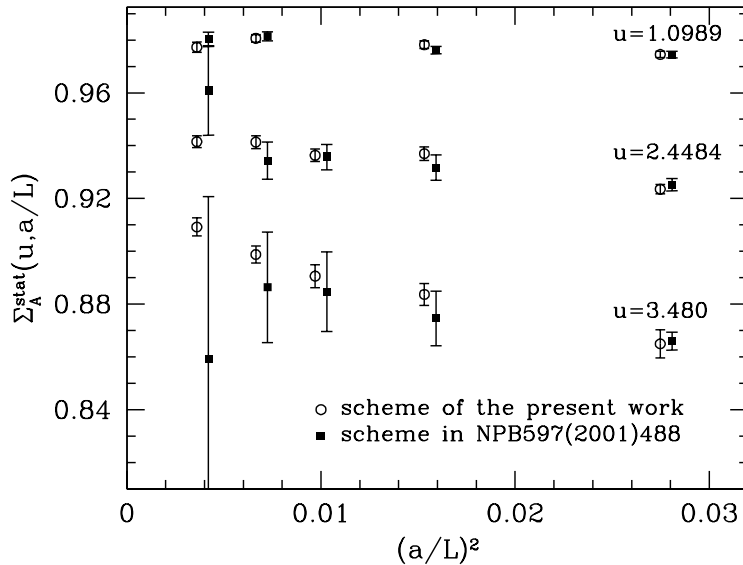


Figure 2: Comparison of the numerical precision of the lattice step scaling function computed in the scheme of Ref. [17] with the new one introduced in Subsection 2.3, which will be used in the rest of this paper. (The symbols are slightly displaced for better readability.) The statistics of both computations is the same.

Z_A^{stat} for $2L/a = 24, 32$), already around $u \approx 1.5$ a precise determination of $\Sigma_A^{\text{stat}}(u, a/L)$ with a reasonable computational effort becomes impossible. The reason for this lies in the boundary correlator f_1^{stat} being part of the renormalization condition Eq. (2.7): it contains the static quark propagating over a distance $T = L$. Thus f_1^{stat} falls roughly like $e^{-e_1 g_0^2 T/a}$ with $e_1 = \frac{1}{12\pi^2} \times 19.95$ [30] the leading coefficient of the self-energy of a static quark. On the other hand, the statistical errors fall much more slowly, leaving us with an exponential degradation of the signal-to-noise ratio.

To circumvent this problem, we now introduce a slightly modified renormalization scheme. (Therefore, for the rest of the paper, the scheme of Ref. [17] — if mentioned at all — will only be referred to by labelling the corresponding quantities with an additional ‘old’, e.g. $Z_A^{\text{stat}} \rightarrow Z_{A,\text{old}}^{\text{stat}}$.) The general idea is to replace f_1^{stat} containing a static and a light quark by two boundary-to-boundary correlation functions. One of them contains a light quark-antiquark pair, the other a static quark-antiquark pair. Both can be computed with small statistical errors, the latter because the variance reduction method of Ref. [31] can be applied. Since the static-static boundary correlator has not been studied before, we discuss it in some detail.

2.2 The static-static boundary correlator f_1^{hh}

We define

$$f_1^{\text{hh}}(x_3) \equiv -\frac{1}{2L^2} \int dx_1 dx_2 d^3\mathbf{y} d^3\mathbf{z} \langle \bar{\zeta}_h'(\mathbf{x}) \gamma_5 \zeta_h'(\mathbf{0}) \bar{\zeta}_h(\mathbf{y}) \gamma_5 \zeta_h(\mathbf{z}) \rangle, \quad (2.11)$$

represented graphically in the left part of Figure 3. After integrating out the static quark fields, f_1^{hh} becomes the (trace of the) product of a timelike Wilson line and the complex

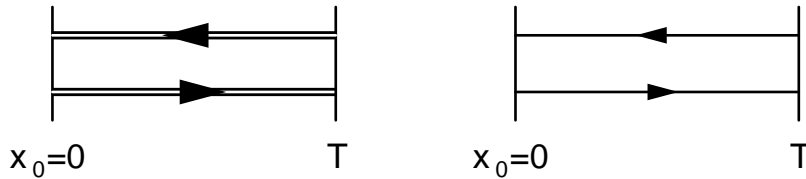


Figure 3: The correlation functions $f_1^{\text{hh}}(x_3)$ (left) and f_1 (right). The notation is the same as in Figure 1.

conjugate one from boundary to boundary (see Eq. (B.1)). They are separated by \mathbf{x} in space. This quantity is integrated over x_1, x_2 but retains a dependence on x_3 . In the following we take $d \equiv |x_3|$ as its argument, where the periodicity of the system in the space directions restricts it to $0 \leq d \leq L/2$.

Upon renormalization the correlation function f_1^{hh} becomes

$$(f_1^{\text{hh}})_R(d) = e^{-2\delta m \times L} (Z_h)^4 f_1^{\text{hh}}(d),$$

where Z_h is the wave function renormalization constant of a static boundary quark field and δm the linearly divergent static mass counterterm. Therefore, to study the properties of f_1^{hh} further, we form the finite ratio

$$h(d/L, u) \equiv \frac{(f_1^{\text{hh}})_R(d)}{(f_1^{\text{hh}})_R(L/2)} = \frac{f_1^{\text{hh}}(d)}{f_1^{\text{hh}}(L/2)} \quad \text{at} \quad \bar{g}^2(L) = u. \quad (2.12)$$

Considered on the lattice, it has a continuum limit. As outlined in Appendix B.1, the one-loop coefficient $h^{(1)}(d/L)$ of the perturbative expansion

$$h(d/L, u) = 1 + u h^{(1)}(d/L) + u^2 h^{(2)}(d/L) + \dots \quad (2.13)$$

is given by

$$h^{(1)}(d/L) = \frac{2}{3} \left(\frac{1}{2} - \frac{d}{L} \right)^2. \quad (2.14)$$

Remarkably, this form holds exactly on the lattice without any a/L -dependence. Some insight why this is so is presented in the appendix as well. At two-loop accuracy, we do not expect exact a -independence any more, but still one may hope that the favourable kinematics keep lattice artifacts small.

The one-loop expression is compared to results from our non-perturbative computation of f_1^{hh} for two representative values of the coupling in Figure 4. The figure contains non-perturbative results for $L/a \in \{12, 16, 20, 24, 32\}$ but at the level of our statistical errors, which are about 1% and smaller, no lattice artifacts of the ratio h can be seen.

For low d , the non-perturbative data for h are well described by $c \times (L/d) + c'$, where the constant c grows with $u = \bar{g}^2$. Hence the correlation function contains a non-integrable short-distance singularity, which is the reason why we will not integrate over d in the following. It is easy to see that this singularity is absent up to and including the order u^2 , but in higher-order terms in perturbation theory such a singularity may appear.

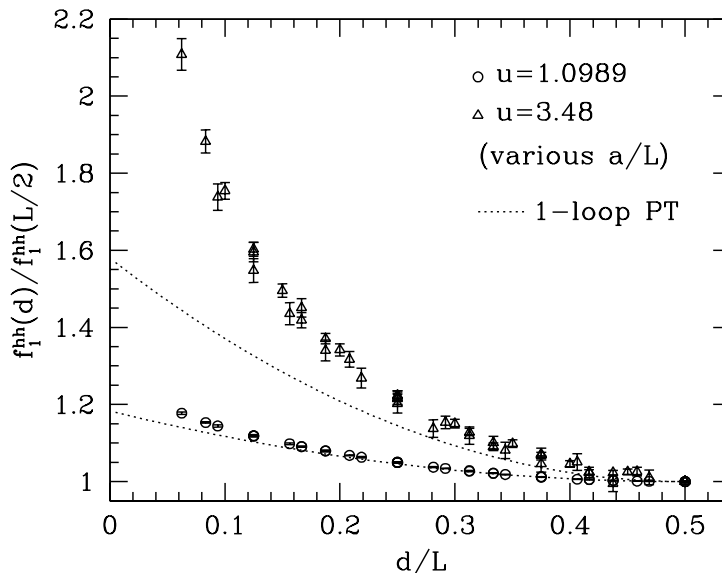


Figure 4: Non-perturbative d -dependence of $h(d/L, u) = f_1^{\text{hh}}(d)/f_1^{\text{hh}}(L/2)$ at two (low and high) values of the coupling, compared to one-loop perturbation theory. As data points corresponding to various lattice resolutions are included, the figure also reflects the weak cutoff dependence of this ratio.

2.3 The new renormalization scheme

Choosing d at its maximum value to further keep discretization errors at a minimum, we specify our (non-perturbative) renormalization scheme by

$$Z_A^{\text{stat}}(L) \Xi(L) = \Xi^{(0)}(L) \quad \text{at vanishing quark mass,} \quad (2.15)$$

with

$$\Xi(L) = \frac{f_A^{\text{stat}}(L/2)}{[f_1 f_1^{\text{hh}}(L/2)]^{1/4}}. \quad (2.16)$$

Here, f_1 is the correlator between two light-quark pseudoscalar boundary sources,

$$f_1 = -\frac{1}{2L^6} \int d^3\mathbf{u} d^3\mathbf{v} d^3\mathbf{y} d^3\mathbf{z} \langle \bar{\zeta}_1'(\mathbf{u}) \gamma_5 \zeta_2'(\mathbf{v}) \bar{\zeta}_2(\mathbf{y}) \gamma_5 \zeta_1(\mathbf{z}) \rangle, \quad (2.17)$$

depicted in the right part of Figure 3. The form of f_1 and f_1^{hh} on the lattice is given in Eqs. (A.12) and (A.14) of Appendix A.1. As before, the combination of these correlators in the denominator of (2.16) is such that the boundary field renormalizations and the mass counterterm drop out and no other scale but L appears.

For $\theta = 0.5$ the perturbative calculation summarized in Appendix B now yields

$$\gamma_1^{\text{SF}} = \frac{1}{(4\pi)^2} \{ 0.10(2) - 0.0477(13) N_f \}, \quad (2.18)$$

which differs only little from the one in the old scheme [17].

Note that $O(a)$ improvement [32, 21] can be applied and is an important ingredient in practice to reduce the cutoff effects in the numerical simulations (see Appendix A). Returning to Figure 2, one observes that the statistical errors of the lattice results are indeed much smaller in the new scheme.

3 Non-perturbative running and renormalization group invariant

In this section we present our quenched results on the evolution of $\Phi(\mu)$ over more than two orders of magnitude in μ . To this end we consider the evolution of $Z_{\text{A}}^{\text{stat}}$ under repeated changes of the scale (i.e. the box size L) by a factor of two at fixed bare parameters. Starting at some initial low-energy value (i.e. some large $L = L_{\text{max}}$), one thereby climbs up the energy scale by repeated application of the inverse of the step scaling function until the perturbative domain at high energies (i.e. small $2^{-k}L_{\text{max}}$) is reached, where finally the associated (scale and scheme independent) renormalization group invariant may be extracted. As in the previous section we keep the discussion in the continuum theory here; the underlying lattice calculations are described in Appendix A.

3.1 Step scaling function

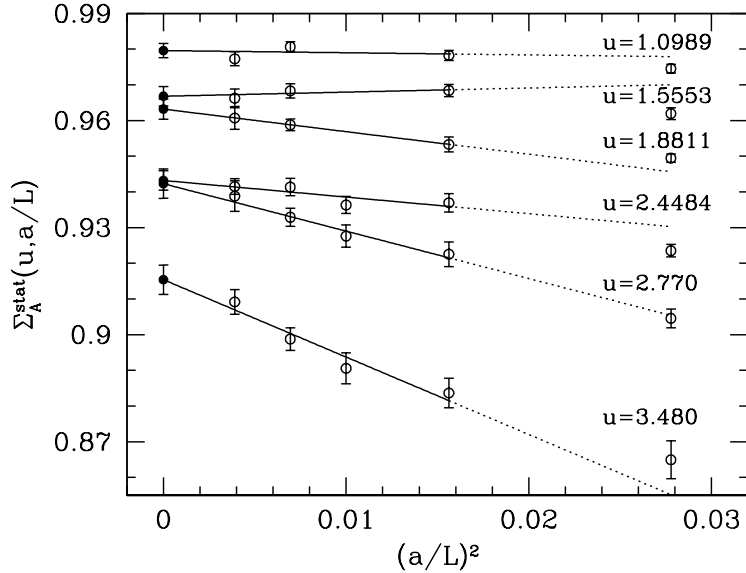


Figure 5: Lattice step scaling function $\Sigma_{\text{A}}^{\text{stat}}$ and its continuum limit extrapolations for some selected values of u .

The evolution of $Z_{\text{A}}^{\text{stat}}$ from size L to $2L$ is given by its step scaling function, $\sigma_{\text{A}}^{\text{stat}}(u)$, which has already been introduced in Eq. (2.6), but where it is understood that $Z_{\text{A}}^{\text{stat}}$ is defined in the new renormalization scheme according to Eq. (2.15).

As detailed in Appendix A.2, the sets of lattice parameters $(L/a, \beta, \kappa)$, which in practice are required to non-perturbatively compute $\sigma_{\text{A}}^{\text{stat}}(u)$, can be taken over from the quark mass renormalization [13]. The available coupling values u allow to trace the scale dependence of $Z_{\text{A}}^{\text{stat}}$ up to $L = 2L_{\text{max}}$, where the scale L_{max} is implicitly defined through

$$\bar{g}^2(L_{\text{max}}) = 3.48. \quad (3.1)$$

The sequence

$$u_k = \bar{g}^2(2^{-k}L_{\text{max}}), \quad k = 0, \dots, 8, \quad (3.2)$$

is known from Ref. [13], and thus the corresponding sequence

$$v_k \equiv \frac{Z_{\text{A}}^{\text{stat}}(2^{-k+1}L_{\text{max}})}{Z_{\text{A}}^{\text{stat}}(2L_{\text{max}})} = \frac{\Phi(2^{k-1}/L_{\text{max}})}{\Phi((2L_{\text{max}})^{-1})}, \quad v_0 = 1, \quad (3.3)$$

is simply given by

$$v_0 = 1, \quad v_{k+1} = \frac{v_k}{\sigma_{\text{A}}^{\text{stat}}(u_k)}, \quad (3.4)$$

once the function $\sigma_{\text{A}}^{\text{stat}}(u)$ is available in the corresponding range of u .

u	$\sigma_{\text{A}}^{\text{stat}}(u)$
1.0989	0.9796(20)
1.3293	0.9746(25)
1.4300	0.9719(26)
1.5553	0.9668(27)
1.6950	0.9727(28)
1.8811	0.9632(28)
2.1000	0.9589(35)
2.4484	0.9432(27)
2.7700	0.9423(41)
3.4800	0.9154(41)

Table 1: Results for the continuum step scaling function $\sigma_{\text{A}}^{\text{stat}}(u)$.

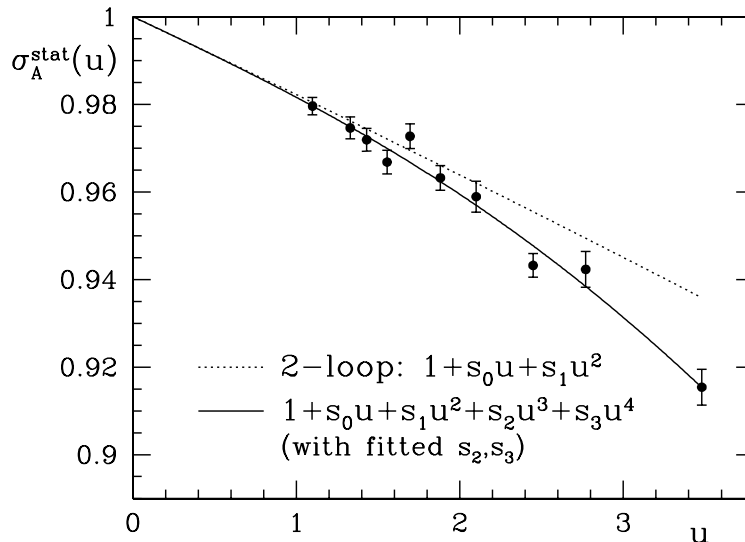


Figure 6: Continuum step scaling function $\sigma_{\text{A}}^{\text{stat}}(u)$ and its polynomial fit.

The calculation of the lattice step scaling function and its subsequent continuum extrapolation yields the pairs u and $\sigma_{\text{A}}^{\text{stat}}(u)$ listed in Table 1. An impression of the quality of the continuum extrapolation is gained from Figure 5, but for a more detailed account of the lattice simulations and data analysis we refer to Appendix A.2. An interpolating fit

of $\sigma_A^{\text{stat}}(u)$ is shown in Figure 6. The leading coefficients (s_0 and s_1 , see Appendix C.1) of the interpolating polynomial are fixed to the perturbative predictions, Eqs. (B.14). This fit is then inserted into the aforementioned recursion, and propagating all errors through the recursion we obtain

$$Z_A^{\text{stat}}(2L_{\text{max}})/Z_A^{\text{stat}}(L) = 0.7551(47) \quad \text{at} \quad L = 2^{-6}L_{\text{max}}, \quad (3.5)$$

with the value of the coupling at this box size being $\bar{g}^2(2^{-6}L_{\text{max}}) = 1.053(12)$ [13]. Let us emphasize once more that $L = 2L_{\text{max}}$ and $L = 2^{-6}L_{\text{max}}$ represent low- and high-energy scales, respectively, which in this way have been connected non-perturbatively. (Our data actually allow to go up to $L = 2^{-8}L_{\text{max}}$.)

3.2 RGI matrix elements of the static axial current

We now proceed to relate the renormalized matrix element

$$\Phi(\mu) = Z_A^{\text{stat}}(L)\Phi_{\text{bare}}(g_0), \quad \mu = 1/L, \quad (3.6)$$

at $L = 2L_{\text{max}}$ to the renormalization group invariant one defined by²

$$\Phi_{\text{RGI}} = \Phi(\mu) \times [2b_0\bar{g}^2(\mu)]^{-\gamma_0/2b_0} \exp \left\{ - \int_0^{\bar{g}(\mu)} dg \left[\frac{\gamma(g)}{\beta(g)} - \frac{\gamma_0}{b_0g} \right] \right\}, \quad (3.7)$$

with the universal leading-order coefficients $b_0 = 11/(4\pi)^2$ and $\gamma_0 = -1/(4\pi^2)$ of the β - and γ -functions, respectively. Casting this equation in the form

$$\begin{aligned} \frac{\Phi_{\text{RGI}}}{\Phi((2L_{\text{max}})^{-1})} &= \frac{Z_A^{\text{stat}}(1/\mu)}{Z_A^{\text{stat}}(2L_{\text{max}})} \\ &\times [2b_0\bar{g}^2(\mu)]^{-\gamma_0/2b_0} \exp \left\{ - \int_0^{\bar{g}(\mu)} dg \left[\frac{\gamma(g)}{\beta(g)} - \frac{\gamma_0}{b_0g} \right] \right\}, \end{aligned}$$

with $\mu = 2^6/L_{\text{max}}$, we see that the first factor is known from Eq. (3.5), while in the second one only couplings $\bar{g}^2 \leq 1.05$ contribute and it can safely be evaluated by perturbation theory. Still, for the perturbative error to be negligible, γ has to be known to two-loop accuracy and β to three-loop. Upon inserting $\bar{g}^2(2^6/L_{\text{max}}) = 1.053$ and numerical integration of the second factor we find

$$\Phi(\mu)/\Phi_{\text{RGI}} = 1.088(8) \quad \text{at} \quad \mu = (2L_{\text{max}})^{-1} \quad (3.8)$$

in the SF scheme. Entirely consistent numbers, with slightly larger errors, are obtained for $\Phi(\mu)/\Phi_{\text{RGI}}$ if one switches to perturbation theory at $\mu = 2^7/L_{\text{max}}$ or $\mu = 2^8/L_{\text{max}}$ instead.

In Figure 7 we compare the numerically computed running with the corresponding curves in perturbation theory. While good agreement with the perturbative approximation is seen at high scales, a growing difference of up to 5% becomes visible when μ is lowered to $\mu \approx 2.5\Lambda$.

Below it will be more convenient to specify the scale μ in Eq. (3.8) in terms of r_0 [33] instead of L_{max} . Taking also the small error contribution from the uncertainty of L_{max} in

²In a loose notation, we take sometimes L and sometimes $\mu = 1/L$ as the argument of \bar{g} .

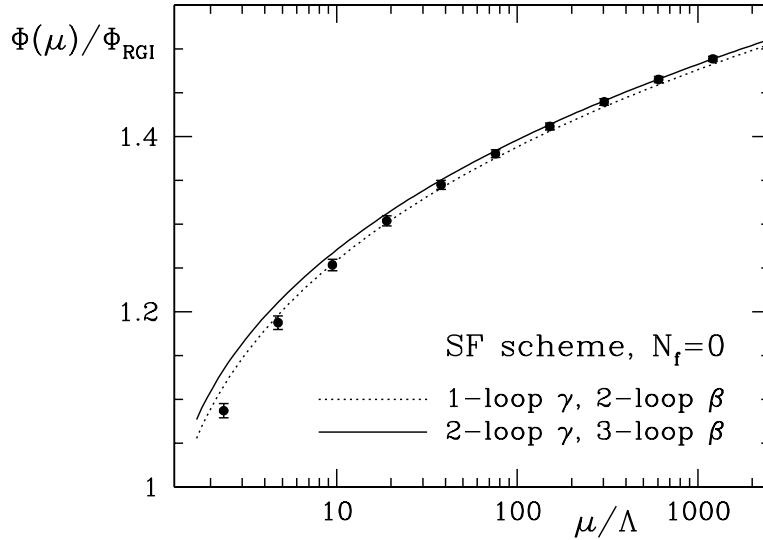


Figure 7: Numerically computed values of the running matrix element of the static axial current in the SF scheme compared to perturbation theory. The dotted and solid lines are obtained from Eq. (3.7) using the 1/2- and 2/3-loop expressions for the γ - and β -functions, respectively, as well as $\Lambda L_{\text{max}} = 0.211$ from Ref. [13].

units of r_0 , $L_{\text{max}}/r_0 = 0.718(16)$ [34], into account, the final result for the regularization independent part $\Phi(\mu)/\Phi_{\text{RGI}}$ of the total renormalization factor is

$$\Phi(\mu)/\Phi_{\text{RGI}} = 1.088(10) \quad \text{at} \quad \mu = (1.436 r_0)^{-1}. \quad (3.9)$$

Note that this result refers to the *continuum limit* so that the error on $\Phi(\mu)/\Phi_{\text{RGI}}$ of about 0.9% should only be added in quadrature to the proper matrix element under study *after* its continuum extrapolation.

4 $Z_{\text{A}}^{\text{stat}}$ at low scale and total renormalization factor

We still need to relate $(A_{\text{R}}^{\text{stat}})_0(\mu)$, renormalized at some appropriate scale μ , to the bare lattice operator. This amounts to computing $Z_{\text{A}}^{\text{stat}}$ at the low-energy matching scale $L = 2L_{\text{max}} = 1.436 r_0$, which is briefly explained in Appendix C.2. Since in this step the bare operator is involved, $Z_{\text{A}}^{\text{stat}}$ does depend — in contrast to the result of the previous section — on the choice of action. We have considered three different cases. The first two are the non-perturbatively $\mathcal{O}(a)$ improved action of Ref. [35], with $c_{\text{A}}^{\text{stat}} = -\frac{1}{4\pi} \times g_0^2$ (= one-loop) and separately with $c_{\text{A}}^{\text{stat}} = 0$. Their combination will in the future allow to study the influence of $c_{\text{A}}^{\text{stat}}$ on the continuum extrapolations of renormalized matrix elements. The third choice is the unimproved Wilson action which is of interest, because so far the best computations of the bare matrix element did not use improvement [10, 11].

The numerical results for $Z_{\text{A}}^{\text{stat}}$ are shown in Figure 8. For later use they are represented by interpolating polynomials,

$$Z_{\text{A}}^{\text{stat}}(g_0, L/a) \Big|_{L=1.436 r_0} = \sum_{i \geq 0} z_i (\beta - 6)^i, \quad (4.1)$$

with coefficients z_i as listed in Table 2. The statistical uncertainty to be taken into account when using this formula is about 0.4%.

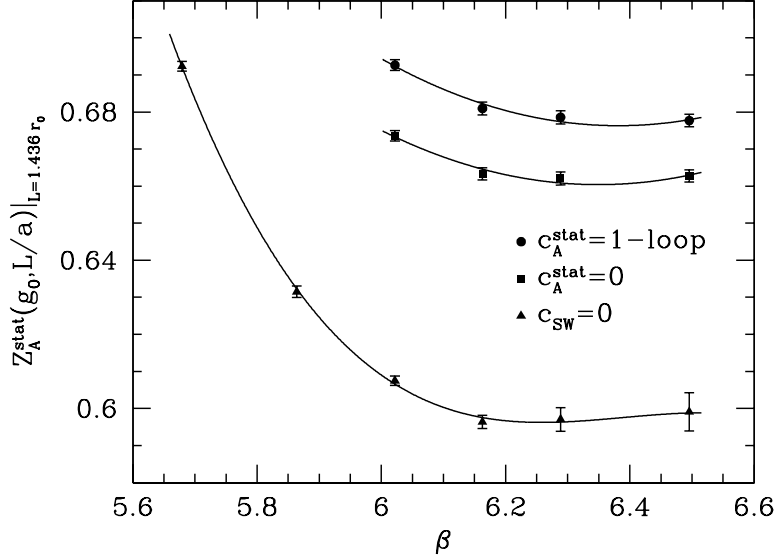


Figure 8: Numerical results for $Z_A^{\text{stat}}(g_0, L/a)|_{L=1.436 r_0}$ together with their interpolating polynomials.

c_{sw}, c_A	c_A^{stat}	applicability	i	z_i	f_i
non-perturbative [35]	$-g_0^2/(4\pi)$	$6.0 \leq \beta \leq 6.5$	0	0.6944	0.6382
			1	-0.0946	-0.0869
			2	0.1239	0.1139
non-perturbative	0	$6.0 \leq \beta \leq 6.5$	0	0.6750	0.6204
			1	-0.0838	-0.0771
			2	0.1200	0.1103
0, 0	0	$5.7 \leq \beta \leq 6.5$	0	0.6090	0.5598
			1	-0.1186	-0.1090
			2	0.3438	0.3160
			3	-0.2950	-0.2711

Table 2: Coefficients of the interpolating polynomials, Eq. (4.1) and Eq. (4.3). Uncertainties are discussed in the text.

The total renormalization factor

The total renormalization factor to directly translate any bare matrix element $\Phi_{\text{bare}}(g_0)$ of A_0^{stat} into the RGI matrix element, Φ_{RGI} , can be written as

$$Z_{\text{RGI}}(g_0) = \frac{\Phi_{\text{RGI}}}{\Phi(\mu)} \Big|_{\mu=(1.436 r_0)^{-1}} \times Z_A^{\text{stat}}(g_0, L/a) \Big|_{L=1.436 r_0}. \quad (4.2)$$

We combine Eq. (4.1) with Eq. (3.9) and represent the total Z -factor by further interpolating polynomials,

$$Z_{\text{RGI}}(g_0) = \sum_{i \geq 0} f_i (\beta - 6)^i, \quad (4.3)$$

whose coefficients are also found in Table 2. These parametrizations of Z_{RGI} are to be used with an uncertainty of about 0.4%³ at each β -value and an additional error of 0.9% (from $\Phi_{\text{RGI}}/\Phi(\mu)$), which remains to be added in quadrature *after* performing a continuum extrapolation.

5 Matrix elements at finite values of the quark mass

In order to use results from the static theory, one still has to relate its renormalization group invariant matrix elements to those in QCD at finite values of the quark mass, m . This step may also be seen as a translation to another scheme, defined by the condition that matrix elements in the static effective theory renormalized in this scheme and at scale $\mu = m$ are the same as those in QCD up to $1/m$ -corrections. This scheme is therefore denoted as the ‘*matching scheme*’ [14]. Below, we will specify precisely which quark mass m is to be taken.

5.1 Conversion to the matching scheme

Let us write the relations for the special case of the matrix element of the axial current between the vacuum and the heavy-light pseudoscalar,

$$\Phi_{\text{RGI}} = Z_{\text{RGI}} \langle \text{PS} | A_0^{\text{stat}} | 0 \rangle. \quad (5.1)$$

We then have

$$F_{\text{PS}} \sqrt{\overline{m}_{\text{PS}}} = \widehat{C}_{\text{PS}}(\overline{m}) \times \Phi_{\text{RGI}} + \mathcal{O}(1/\overline{m}), \quad (5.2)$$

where \overline{m} is the $\overline{\text{MS}}$ quark mass at renormalization scale \overline{m} .⁴ The function $\widehat{C}_{\text{PS}}(\mu)$ is given by

$$\widehat{C}_{\text{PS}}(\mu) = [2b_0 \overline{g}^2(\mu)]^{\gamma_0/2b_0} \exp \left\{ \int_0^{\overline{g}(\mu)} dg \left[\frac{\gamma(g)}{\beta(g)} - \frac{\gamma_0}{b_0 g} \right] \right\}, \quad (5.3)$$

with $\overline{g}(\mu)$ the $\overline{\text{MS}}$ running coupling and γ the anomalous dimension in the matching scheme. The latter is known to two loops [38, 39, 40, 30] with γ_0 being the same as before and

$$\gamma_1 \equiv \gamma_1^{\text{match}} = \gamma_1^{\overline{\text{MS}}} - \frac{b_0}{3\pi^2}, \quad (5.4)$$

$$\gamma_1^{\overline{\text{MS}}} = -\frac{1}{576\pi^4} \left(\frac{127}{2} + 28\zeta(2) - 5N_f \right). \quad (5.5)$$

For illustration, $\widehat{C}_{\text{PS}}(\mu)$ is plotted in the upper part of Figure 9, where for the numerical evaluation the β -function is always taken at four-loop precision [41], while to estimate the

³Only in the case $c_{\text{sw}} = 0$ the error to be associated with the formulae for $Z_{\text{A}}^{\text{stat}}$ and Z_{RGI} grows to 0.5% at $\beta \approx 6.3$ and 0.8% at $\beta \approx 6.5$.

⁴Note that in [36] a similar equation with the pole mass instead of the $\overline{\text{MS}}$ mass is written. At the two-loop order, which will be used below, this does formally not make any difference. However, the pole mass does not have a well-behaved perturbative expansion [37], and we therefore prefer a short-distance mass such as the $\overline{\text{MS}}$ mass.

perturbative uncertainty we show the result for the one-loop and the two-loop approximation of γ .

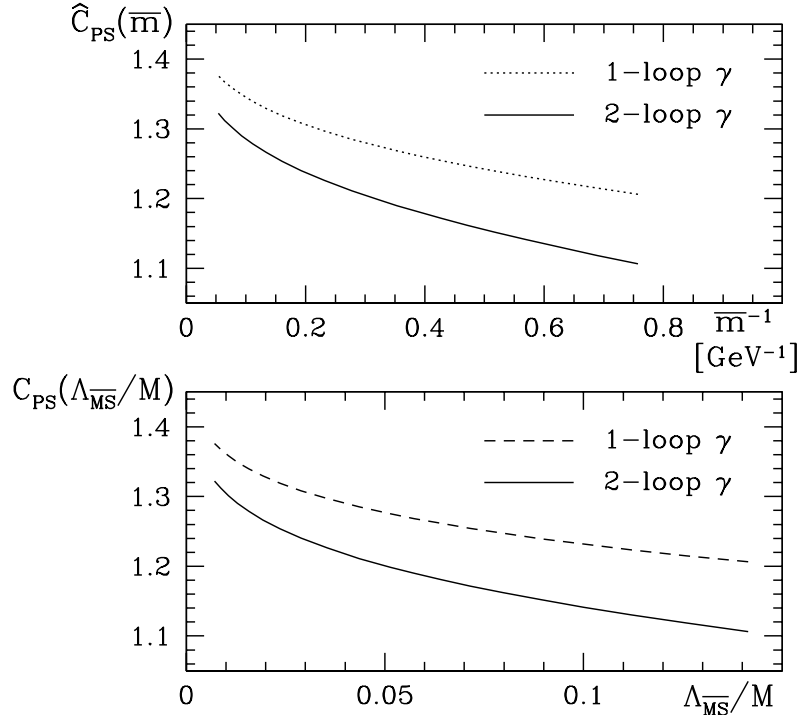


Figure 9: Conversion factor to the matching scheme, which translates the RGI matrix element to the one at finite mass.

Eq. (5.3) can be rewritten in a form displaying explicitly that also this step is not restricted to perturbation theory. In terms of the renormalization group invariant quark mass, M , we have

$$F_{\text{PS}}\sqrt{m_{\text{PS}}} = C_{\text{PS}}(M/\Lambda_{\overline{\text{MS}}}) \times \Phi_{\text{RGI}} + \mathcal{O}(1/M), \quad (5.6)$$

where now only renormalization group invariants enter. To evaluate $C_{\text{PS}}(M/\Lambda_{\overline{\text{MS}}})$ in perturbative approximation, one changes the argument of the function \hat{C}_{PS} , Eq. (5.3), by inserting

$$M/\bar{m}(\mu) = [2b_0\bar{g}^2(\mu)]^{-d_0/2b_0} \exp \left\{ - \int_0^{\bar{g}(\mu)} dg \left[\frac{\tau(g)}{\beta(g)} - \frac{d_0}{b_0g} \right] \right\} \quad (5.7)$$

together with the condition $\bar{m}(m_{\overline{\text{MS}}}) = m_{\overline{\text{MS}}}$, where $\tau(\bar{g})$ denotes as usual the renormalization group function of the renormalized (running) quark mass with universal leading-order coefficient $d_0 = 8/(4\pi)^2$. A numerical evaluation (with the four-loop τ -function [42, 43] in Eq. (5.7)) is shown in the lower part of Figure 9. Eq. (5.6) is not only the cleanest form from a theoretical point of view but it is also practical, because the relation between bare quark masses in the $\mathcal{O}(a)$ improved lattice theory and the renormalization group invariant mass M is known non-perturbatively in the quenched approximation [44, 45].

For later convenience we represent C_{PS} in terms of the variable $x \equiv 1/\ln(M/\Lambda_{\overline{\text{MS}}})$ in a functional form motivated by Eq. (5.3),

$$C_{\text{PS}} = x^{\gamma_0/2b_0} \{ 1 - 0.065x + 0.048x^2 \}, \quad x = 1/\ln(M/\Lambda_{\overline{\text{MS}}}) \leq 0.52, \quad (5.8)$$

with $b_0 = 11/(4\pi)^2$ and $\gamma_0 = -1/(4\pi^2)$. It describes the result for the two-loop approximation of the γ -function within less than 0.01%. Of course in this step a perturbative error is involved, which is difficult to estimate. Assuming a geometric growth of the coefficients of the γ -function, we find that the γ_2 -term would cause a change by around 1% at $\bar{m} = m_{b,\overline{\text{MS}}}$ and by 2.5% at $\bar{m} = 1.2 \text{ GeV}$. Thus one may attribute a 2–4% error due to the perturbative approximation, which could be much reduced by a computation of the three-loop anomalous dimension.

In principle, C_{PS} may be computed also non-perturbatively following the strategy outlined in Ref. [14]. It is then defined only up to $1/M$ -terms, consistent with Eq. (5.6).

5.2 Application: first non-perturbative renormalization of $F_{\text{B}_s}^{\text{stat}}$

We now take bare matrix elements of A_0^{stat} for unimproved Wilson fermions from the literature to obtain an estimate for F_{B_s} in the static approximation. This exercise serves mainly to illustrate how to use our results.

1. The matrix elements are needed at a fixed value of the light quark mass. To avoid issues in the extrapolation to very light quarks, we here consider only F_{B_s} . To fix the strange quark mass, we use that the sum of the light quark masses is to a good approximation proportional to the squared (light-light) pseudoscalar masses, $m_{\text{PS}}^2(1,1)$ [44], and interpolate the data for the decay constant of [10, 11] as a function of $m_{\text{PS}}^2(1,1)r_0^2$ to $m_{\text{PS}}^2(s,s)r_0^2 = (2m_{\text{K}}^2 - m_{\pi}^2)r_0^2 = 2m_{\text{K}}^2r_0^2/(1 + m_l/m_s) = 3.0233$. (To arrive at the latter, we employed $m_{\text{K}}^2r_0^2 = 1.5736$ [44] and $m_s/m_l = 24.4$ from chiral perturbation theory [46].) The resulting dimensionless numbers $r_0^{3/2}\Phi_{\text{bare}}$ are listed in Table 3.

$\beta = 6/g_0^2$	5.7	5.9	6.0	6.1	6.3
r_0/a	2.93(1)	4.48(2)	5.37(2)	6.32(3)	8.49(4)
$r_0^{3/2}\Phi_{\text{bare}}$	4.75(25)	4.09(21)	3.94(13)	3.79(36)	4.00(29)
$r_0^{3/2}\Phi_{\text{RGI}}$	2.99(16)	2.35(12)	2.21(7)	2.09(20)	2.20(16)

Table 3: Matrix elements of A_0^{stat} in units of r_0 for the light quark mass equal to the strange quark mass. Bare matrix elements come from Ref. [10], with the exception of $\beta = 6.0$ which is taken from Ref. [11]. The scale r_0/a [33] is used as determined in Ref. [34], and its uncertainty is already included here.

2. We renormalize by multiplying with Eq. (4.3), using the f_i from Table 2 ($c_{\text{sw}} = c_{\text{A}} = c_{\text{A}}^{\text{stat}} = 0$), take into account a 0.4–0.5% error from the non-universal part of the Z -factor at each value of g_0 and find the last line in Table 3. Assuming the leading linear behaviour in the lattice spacing to dominate for $a/r_0 < 1/4$, we extrapolate to the continuum limit as shown in Figure 10. Adding to the extrapolation error in quadrature also the 0.9% error contribution of Z_{RGI} , which is independent of g_0 , yields

$$r_0^{3/2}\Phi_{\text{RGI}} = 1.93(34) \quad \text{at} \quad a = 0. \quad (5.9)$$

3. Finally, inserting $M_b r_0 = 17.6(5)$ [47, 14] and $\Lambda_{\overline{\text{MS}}} r_0 = 0.602(48)$ [13], one gets via the formula in Eq. (5.8)

$$C_{\text{PS}}(M_b/\Lambda_{\overline{\text{MS}}}) = 1.23(3), \quad (5.10)$$

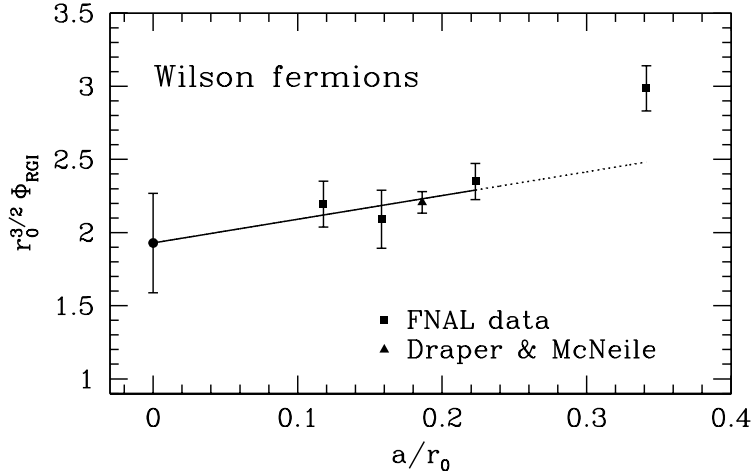


Figure 10: Continuum extrapolation of the non-perturbatively renormalized matrix element of A_0^{stat} based on the unimproved Wilson data for F_B^{bare} from Refs. [10, 11].

where a 2% error for the perturbative approximation is assumed. With the experimental spin-averaged B-meson mass $m_B = m_{B_s} = 5.4 \text{ GeV}$, we then obtain from Eq. (5.6):

$$F_{B_s}^{\text{stat}} r_0 = 0.64(11), \quad (5.11)$$

$$F_{B_s}^{\text{stat}} = 253(45) \text{ MeV} \quad \text{for} \quad r_0 = 0.5 \text{ fm}. \quad (5.12)$$

The result contains all errors apart from the uncertainty owing to the quenched approximation. Evidently, the continuum extrapolation may be done much better, once $O(a)$ improved results with sufficient precision and small lattice spacings are available.

6 Discussion

We have performed the scale dependent renormalization of A_0^{stat} by constructing a non-perturbative renormalization group in the Schrödinger functional scheme, and agreement with perturbation theory at large scales was demonstrated. The renormalization factors needed to extract the associated RG invariant are computed with good numerical accuracy, which is a crucial prerequisite for a controlled determination of F_B in the static limit. In Ref. [14] it was shown that the renormalization factors obtained in this way differ appreciably from earlier estimates [10] based on tadpole-improved perturbation theory [48]. Hence their non-perturbative computation is important.

We have not emphasized this so far, but our computation provides the scale dependence of *all* static-light bilinears

$$\mathcal{O}_\Gamma(x) = \bar{\psi}_1(x) \Gamma \psi_h(x). \quad (6.1)$$

They are renormalized by

$$\begin{aligned} (\mathcal{O}_{\gamma_k})_{\text{R}}(x) &= Z_A^{\text{stat}} \mathcal{O}_{\gamma_k}, \\ (\mathcal{O}_{\gamma_0})_{\text{R}}(x) &= \tilde{Z} Z_A^{\text{stat}} \mathcal{O}_{\gamma_0}, \quad (\mathcal{O}_{\gamma_k \gamma_5})_{\text{R}}(x) = \tilde{Z} Z_A^{\text{stat}} \mathcal{O}_{\gamma_k \gamma_5}, \end{aligned} \quad (6.2)$$

with a scale independent renormalization \tilde{Z} . This pattern is due to the heavy quark spin symmetry which is exact on the lattice, and due to the chiral symmetry of the continuum

theory. The latter means that the relative renormalization \tilde{Z} may be fixed by imposing a suitable chiral Ward identity [49] and is thus scale independent.

Returning to the case of most interest, F_B^{stat} , our continuum extrapolation in Section 5.2 that uses unimproved data for the bare matrix elements from the literature and also quite large lattice spacings leaves much room for improvement of the present result, $F_{B_s}^{\text{stat}} = 253(45)$ MeV. Apart from the obvious step of obtaining $O(a)$ improved bare matrix elements at small lattice spacings and extrapolating to the continuum, it will be necessary to estimate the $O(1/M)$ correction. There are two possible roads towards this goal.

An elegant and clean way is to compute the $1/M$ -corrections directly as perturbations to the static effective theory. Again, the main problem here is renormalization. Indeed, this is a severe one, since mixing between operators of different dimensions has to be taken into account. This will require much more theoretical and numerical effort; but a possible strategy exists [47, 14].

In the mean time, one may also compare the prediction from the static approximation to what one obtains at $M \approx M_c$ and also to the results obtained directly at $M = M_b$, most notably the ones of Refs. [2, 3]. As emphasized in Refs. [50, 51, 52] this should be done in the continuum limit, since $O(a)$ errors get enhanced when the quark masses increase. At the charm quark mass these are sizeable but can be extrapolated away, at least in the quenched approximation [53]. The comparison between finite-mass decay constants and F_B^{stat} is most conveniently done by comparing $F_{\text{PS}}\sqrt{m_{\text{PS}}}/C_{\text{PS}}(M/\Lambda_{\overline{\text{MS}}})$. Unfortunately, at present the error of the static result is still too large to draw any strong conclusions about $1/M$ -corrections in F_B :

$$r_0^{3/2} \Phi_{\text{RGI}} = 1.93(34), \quad \text{static : Eq. (5.9)}, \quad (6.3)$$

$$r_0^{3/2} \frac{F_{B_s}\sqrt{m_{B_s}}}{C_{\text{PS}}(M_b/\Lambda_{\overline{\text{MS}}})} = 1.46(23), \quad \text{using } F_{B_s} = 192(30) \text{ MeV [2, 3]}, \quad (6.4)$$

$$r_0^{3/2} \frac{F_{D_s}\sqrt{m_{D_s}}}{C_{\text{PS}}(M_c/\Lambda_{\overline{\text{MS}}})} = 1.29(5), \quad \text{using } F_{D_s} = 252(9) \text{ MeV [54]}. \quad (6.5)$$

Still, the difference of Eq. (6.3) and Eq. (6.5) shows that there are significant $1/M$ -corrections in the charm mass region.

As a more technical remark we point out that the function $h(d/L, u)$, Eq. (2.12), shows very small a -effects in the quenched approximation and may be worth studying to verify improvement with dynamical fermions.

Acknowledgements

We thank DESY for allocating computer time on the APE-Quadrics computers at DESY Zeuthen to this project. This work is also supported in part by the EU IHP Network on *Hadron Phenomenology from Lattice QCD* under grant HPRN-CT-2000-00145 and by the DFG Sonderforschungsbereich SFB/TR 9.

Appendix A Computation of the lattice step scaling function

This appendix describes some details of the numerical simulations on the lattice and the subsequent calculations that we have performed in order to determine the step scaling function for Z_A^{stat} . At the beginning we also recall a few basic definitions and formulae, which

are specific to the inclusion of static quarks and the correlation functions that are considered in the framework of the Schrödinger functional (SF). As the impact of the static quarks on $O(a)$ improvement of the static-light sector has extensively been discussed in Ref. [17], the reader might consult this reference for further details and any unexplained notation.

A.1 Definitions

Lattice action

The total lattice action is given by the sum

$$S[U, \bar{\psi}_1, \psi_1, \bar{\psi}_h, \psi_h] = S_G[U] + S_F[U, \bar{\psi}_1, \psi_1] + S_h[U, \bar{\psi}_h, \psi_h], \quad (\text{A.1})$$

where S_G and S_F are the standard pure gauge and $O(a)$ improved Wilson actions for relativistic (light) quarks, see Eqs. (A.22) and (A.23) – (A.26) of Ref. [17], respectively, and S_h denotes the lattice action for the heavy quark:

$$S_h[U, \bar{\psi}_h, \psi_h] = a^4 \sum_x \bar{\psi}_h(x) \nabla_0^* \psi_h(x). \quad (\text{A.2})$$

The fields ψ_h and $\bar{\psi}_h$ of the static effective theory are constrained in such a way (namely $P_+ \psi_h = \psi_h$ and $\bar{\psi}_h P_+ = \bar{\psi}_h$) that one is left with just two degrees of freedom per space-time point [4] and only the (time component of the) backward lattice derivative, ∇_μ^* , enters in the action (A.2). Hence, static quarks propagate only forward in time, which also reflects in the form of the associated quark propagator,

$$S_h(x, y) = U(x - a\hat{0}, 0)^{-1} U(x - 2a\hat{0}, 0)^{-1} \dots U(y, 0)^{-1} \\ \times \theta(x_0 - y_0) \delta(\mathbf{x} - \mathbf{y}) P_+, \quad P_\pm = \frac{1}{2} (1 \pm \gamma_0), \quad (\text{A.3})$$

being just a straight timelike Wilson line.

To impose SF boundary conditions, Eqs. (A.1) and (A.2) are supplemented by

$$\begin{aligned} \psi_1(x) &= 0 && \text{if } x_0 < 0 \text{ or } x_0 > L, \\ \psi_h(x) &= 0 && \text{if } x_0 < 0 \text{ or } x_0 \geq L \end{aligned} \quad (\text{A.4})$$

and

$$P_- \psi_1(x) \Big|_{x_0=0} = P_+ \psi_1(x) \Big|_{x_0=L} = 0, \quad (\text{A.5})$$

while in the pure gauge part the spatial plaquettes at $x_0 = 0$ and $x_0 = L$ receive a non-trivial (and coupling dependent) weight, see Eq. (A.29) of Ref. [17]. In the discretization of the SF as described in [18, 21] we choose zero boundary gauge fields throughout, $C = C' = 0$, which translates into the boundary conditions $U(x, k)|_{x_0=0} = U(x, k)|_{x_0=L} = 1$ for the lattice gauge field. Similarly, the light and static quark fields at $x_0 = 0, L$ are fixed to appropriate (space dependent) boundary functions; the corresponding boundary conditions are collected in Eqs. (3.2), (3.3) and (3.5) of Ref. [17] and not repeated here.

SF correlation functions

Observables are then defined as usual through a path integral involving the total action S . In this work we focus on SF correlation functions that are constructed from the $O(a)$ improved static-light axial current

$$(A_I^{\text{stat}})_0(x) = A_0^{\text{stat}}(x) + ac_A^{\text{stat}} \delta A_0^{\text{stat}}(x), \quad (\text{A.6})$$

$$A_0^{\text{stat}}(x) = \bar{\psi}_1(x) \gamma_0 \gamma_5 \psi_h(x), \quad (\text{A.7})$$

$$\delta A_0^{\text{stat}}(x) = \bar{\psi}_1(x) \gamma_j \gamma_5 \frac{1}{2} \left(\overleftarrow{\nabla}_j + \overleftarrow{\nabla}_j^* \right) \psi_h(x). \quad (\text{A.8})$$

Unless it is indicated differently, the improvement coefficient c_A^{stat} is set to its one-loop perturbative value,

$$c_A^{\text{stat}} = -\frac{1}{4\pi} g_0^2, \quad (\text{A.9})$$

computed in Refs. [55,56]. On the lattice, in terms of the boundary quark fields $\zeta, \dots, \bar{\zeta}'$, the correlation functions of these fields, as well as the various types of pseudoscalar correlators from one boundary to the other that are needed in addition, read explicitly:

$$f_A^{\text{stat}}(x_0) = -a^6 \sum_{\mathbf{y}, \mathbf{z}} \frac{1}{2} \langle A_0^{\text{stat}}(x) \bar{\zeta}_h(\mathbf{y}) \gamma_5 \zeta_l(\mathbf{z}) \rangle, \quad (\text{A.10})$$

$$f_{\delta A}^{\text{stat}}(x_0) = -a^6 \sum_{\mathbf{y}, \mathbf{z}} \frac{1}{2} \langle \delta A_0^{\text{stat}}(x) \bar{\zeta}_h(\mathbf{y}) \gamma_5 \zeta_l(\mathbf{z}) \rangle, \quad (\text{A.11})$$

$$f_1 = -\frac{a^{12}}{L^6} \sum_{\mathbf{u}, \mathbf{v}, \mathbf{y}, \mathbf{z}} \frac{1}{2} \langle \bar{\zeta}_i'(\mathbf{u}) \gamma_5 \zeta_j'(\mathbf{v}) \bar{\zeta}_j(\mathbf{y}) \gamma_5 \zeta_i(\mathbf{z}) \rangle, \quad (\text{A.12})$$

$$f_1^{\text{stat}} = -\frac{a^{12}}{L^6} \sum_{\mathbf{u}, \mathbf{v}, \mathbf{y}, \mathbf{z}} \frac{1}{2} \langle \bar{\zeta}_l'(\mathbf{u}) \gamma_5 \zeta_h'(\mathbf{v}) \bar{\zeta}_h(\mathbf{y}) \gamma_5 \zeta_l(\mathbf{z}) \rangle, \quad (\text{A.13})$$

$$f_1^{\text{hh}}(x_3) = -\frac{a^8}{L^2} \sum_{x_1, x_2, \mathbf{y}, \mathbf{z}} \frac{1}{2} \langle \bar{\zeta}_h'(\mathbf{x}) \gamma_5 \zeta_h'(\mathbf{0}) \bar{\zeta}_h(\mathbf{y}) \gamma_5 \zeta_h(\mathbf{z}) \rangle. \quad (\text{A.14})$$

Moreover we introduce the two ratios

$$X_I(g_0, L/a) = \frac{f_A^{\text{stat}}(L/2) + ac_A^{\text{stat}} f_{\delta A}^{\text{stat}}(L/2)}{\sqrt{f_1^{\text{stat}}}}, \quad (\text{A.15})$$

$$\Xi_I(g_0, L/a) = \frac{f_A^{\text{stat}}(L/2) + ac_A^{\text{stat}} f_{\delta A}^{\text{stat}}(L/2)}{[f_1 f_1^{\text{hh}}(L/2)]^{1/4}}, \quad (\text{A.16})$$

which are constructed such that the (unknown) wave function renormalization factors of the boundary quark fields as well as the (linearly divergent) mass counterterm δm cancel out and only the static current remains subject to renormalization.

Renormalization

In Ref. [17] the renormalization constant $Z_A^{\text{stat}} \equiv Z_{A, \text{SF}}^{\text{stat}}$ entering the $O(a)$ improved static axial current renormalized in the SF scheme,

$$(A_R^{\text{stat}})_0 = Z_A^{\text{stat}} (1 + b_A^{\text{stat}} am_q) (A_I^{\text{stat}})_0, \quad (\text{A.17})$$

was defined in terms of the ratio Eq. (A.15) by imposing the renormalization condition (with m_0 , m_q and m_c as defined in [17])

$$Z_{A,\text{old}}^{\text{stat}}(g_0, L/a) X_I(g_0, L/a) = X_I(0, L/a) \quad \text{at} \quad m_0 = m_c. \quad (\text{A.18})$$

Thus, $Z_{A,\text{old}}^{\text{stat}}$ naturally runs with the scale $\mu = 1/L$. In the present context it will be referred to as the ‘old’ scheme, whereas the so-called ‘new’ scheme based on Eq. (A.16) is specified by

$$Z_A^{\text{stat}}(g_0, L/a) \Xi_I(g_0, L/a) = \Xi_I(0, L/a), \quad m_0 = m_c, \quad L = 1/\mu. \quad (\text{A.19})$$

For $\theta = 0.5$, which is chosen in our simulations, the relevant values of the tree-level normalization constant $\Xi_I(0, L/a)$ (or $\Xi_I^{(0)}(a/L)$ in the notation of Appendix B summarizing the perturbative calculations) are collected in Table A.1. As an aside we remark that $\Xi_I(0, L/a) = X_I(0, L/a)$ holds.

L/a	$\Xi_I(0, L/a)$
6	-1.5964837518021
8	-1.5996643156321
10	-1.6011462370857
12	-1.6019540566018
16	-1.6027594410020
20	-1.6031330222299
24	-1.6033361949926
32	-1.6035384024722

Table A.1: The ratio Ξ_I for $\theta = 0.5$ at tree-level.

The critical quark mass is always understood to be defined from the non-perturbatively $O(a)$ improved PCAC mass in the light quark sector as in Ref. [13] (i.e. for $\theta = 0$ and $T = L$, evaluating the associated combination of correlation functions at $x_0 = T/2$).

Lattice step scaling function

The lattice step scaling function of the static axial current is defined through

$$\Sigma_A^{\text{stat}}(u, a/L) = \frac{Z_A^{\text{stat}}(g_0, 2L/a)}{Z_A^{\text{stat}}(g_0, L/a)} \quad \text{at} \quad \bar{g}^2(L) = u, m_0 = m_c. \quad (\text{A.20})$$

The additional condition $m_0 = m_c$ from above, referring to lattice size L/a , defines the critical hopping parameter value, $\kappa = \kappa_c$. Moreover, enforcing $\bar{g}^2(L)$ to take some prescribed value u fixes the bare coupling value $g_0^2 = 6/\beta$ to be used for given L/a . In this way Σ_A^{stat} becomes a function of the renormalized coupling u , up to cutoff effects, and approaches its continuum limit as $a/L \rightarrow 0$ for fixed u .

A.2 Simulation details and results

As emphasized before, our quenched lattice simulation and the data analysis are analogous to Ref. [13], except that the boundary coefficient c_t is set to its two-loop perturbative value [57]:

$$c_t^{2\text{-loop}} = 1 - 0.089 g_0^2 - 0.030 g_0^4. \quad (\text{A.21})$$

The boundary $O(a)$ improvement terms involving quark fields have to be multiplied with a coefficient \tilde{c}_t , which is known to one-loop from [58], viz.

$$\tilde{c}_t^{1\text{-loop}} = 1 - 0.018 g_0^2. \quad (\text{A.22})$$

Of course, owing to a priori unknown precision to which perturbation theory approximates these coefficients, linear lattice spacing errors are not suppressed completely, and we will come back to this issue later. As for the other contributing $O(a)$ improvement coefficients, we used the non-perturbative values for c_{sw} and c_A of [35] for the relativistic fermions and the one-loop estimate (A.9) for c_A^{stat} in the static-light axial current.

The renormalization constants $Z_A^{\text{stat}}(g_0, L/a)$ and $Z_A^{\text{stat}}(g_0, 2L/a)$ in Eq. (A.20) have been evaluated from the correlation functions in Eqs. (A.10) – (A.14), which were computed in a numerical simulation with $\theta = 0.5$. (The latter parameter specifies the boundary conditions of the quark fields, see e.g. [20].) These simulations were performed on the APE-100 parallel computers with 128 to 512 nodes, employing for the updating of the gauge fields the same hybrid-overrelaxation algorithm as in [24, 13] with two overrelaxation sweeps per heatbath sweep within a full iteration. This mix of updating was found to be close to optimal in [59]. Since the computation of SF correlators has already been detailed in Refs. [35] and (Appendix A.2.2 of) [13], we just mention that we differ from them only by using the implementation [60] of the SSOR-preconditioned BiCGStab inverter [61] to solve the lattice Dirac equation.

The computation of $f_1^{\text{hh}}(d)$, where $d = |x_3|$ and $a \leq d \leq L/2$, amounts to evaluate Eq. (B.1). In order to improve the statistical precision of f_1^{hh} , the links building up the observable are evaluated by a 10-hit multi-hit procedure [31], where each hit consists of a Cabibbo-Marinari heatbath update in three $SU(2)$ -subgroups of $SU(3)$. Translation invariance is fully exploited.

In order to keep autocorrelations small, the measurements of the correlation functions were always separated by $L/(2a)$ update iterations (and, respectively, five iterations in the case of f_1^{hh}). Statistical errors stem from a standard jackknife analysis, where we have checked explicitly for the statistical independence of the data by averaging them into bins of a few consecutive measurements beforehand. The total number of measurements itself was such that the statistical error of Σ_A^{stat} was dominated by the uncertainty in $Z_A^{\text{stat}}(g_0, 2L/a)$. In general, the uncertainties in the coupling and in the value of κ_c would have to be propagated into the error of Σ_A^{stat} as well. But as the former can be estimated to be much smaller than the statistical error of Σ_A^{stat} and Σ_A^{stat} is found to depend rather weakly on the bare (light) quark mass, we neglected both contributions in the final error estimate.

In Table A.2 – Table A.4 we list our results on the step scaling functions of the static axial current⁵ and — since they are available from our computations as well — of the pseudoscalar density defined as in [13]. The values of β and the critical hopping parameter $\kappa = \kappa_c$ to be simulated were taken over from Ref. [13] without changes, which means to stay with c_t and \tilde{c}_t to one-loop accuracy in realizing the conditions $\bar{g}^2(L) = u$ and $m_0 = m_c$. Note once more, however, that here, in contrast to [13], for the corresponding renormalization constants themselves — particularly when comparing the results for Z_P and Σ_P quoted in that previous work with those of the present one — the two-loop formula for c_t , Eq. (A.21), has been used.

⁵Here we do not tabulate the results on the static-static boundary correlator f_1^{hh} separately, but the numbers can be obtained from the authors upon request.

$\bar{g}^2(L)$	β	κ	L/a	$Z_P(g_0, L/a)$	$Z_P(g_0, 2L/a)$	$\Sigma_P(u, a/L)$
1.0989	9.5030	0.131514	6	0.8190(10)	0.7846(9)	0.9581(16)
	9.7500	0.131312	8	0.8107(9)	0.7786(12)	0.9604(18)
	10.0577	0.131079	12	0.8012(6)	0.7702(11)	0.9613(16)
	10.3419	0.130876	16	0.7956(8)	0.7625(15)	0.9584(21)
1.3293	8.6129	0.132380	6	0.7930(10)	0.7493(10)	0.9449(17)
	8.8500	0.132140	8	0.7827(11)	0.7402(11)	0.9456(19)
	9.1859	0.131814	12	0.7737(7)	0.7353(12)	0.9503(17)
	9.4381	0.131589	16	0.7666(11)	0.7274(18)	0.9488(27)
1.4300	8.5598	0.132453	8	0.7702(10)	0.7273(13)	0.9443(21)
	8.9003	0.132095	12	0.7610(6)	0.7223(14)	0.9491(21)
	9.1415	0.131855	16	0.7555(7)	0.7123(20)	0.9428(28)
1.5553	7.9993	0.133118	6	0.7666(7)	0.7165(16)	0.9346(23)
	8.2500	0.132821	8	0.7590(8)	0.7134(13)	0.9399(20)
	8.5985	0.132427	12	0.7473(10)	0.7035(13)	0.9414(21)
	8.8323	0.132169	16	0.7421(9)	0.6976(19)	0.9401(29)
1.6950	7.9741	0.133179	8	0.7442(11)	0.6939(15)	0.9325(24)
	8.3218	0.132756	12	0.7341(7)	0.6862(15)	0.9348(22)
	8.5479	0.132485	16	0.7277(13)	0.6805(18)	0.9352(30)
1.8811	7.4082	0.133961	6	0.7348(9)	0.6764(6)	0.9205(14)
	7.6547	0.133632	8	0.7258(7)	0.6691(15)	0.9219(23)
	7.9993	0.133159	12	0.7173(5)	0.6632(8)	0.9245(12)
	8.2415	0.132847	16	0.7117(13)	0.6604(20)	0.9279(33)
2.1000	7.3632	0.134088	8	0.7088(13)	0.6433(16)	0.9076(28)
	7.6985	0.133599	12	0.6971(8)	0.6385(24)	0.9160(36)
	7.9560	0.133229	16	0.6919(12)	0.6303(17)	0.9110(29)
2.4484	6.7807	0.134994	6	0.6845(10)	0.6110(12)	0.8925(21)
	7.0197	0.134639	8	0.6784(8)	0.6061(19)	0.8933(30)
	7.2025	0.134380	10	0.6733(8)	0.6021(12)	0.8943(21)
	7.3551	0.134141	12	0.6722(11)	0.6012(12)	0.8944(24)
	7.6101	0.133729	16	0.6661(5)	0.5962(10)	0.8950(17)
2.7700	6.5512	0.135327	6	0.6619(10)	0.5758(20)	0.8699(33)
	6.7860	0.135056	8	0.6541(13)	0.5751(17)	0.8792(31)
	6.9720	0.134770	10	0.6505(8)	0.5717(17)	0.8788(28)
	7.1190	0.134513	12	0.6482(9)	0.5705(10)	0.8802(19)
	7.3686	0.134114	16	0.6442(16)	0.5668(16)	0.8798(33)
3.4800	6.2204	0.135470	6	0.6173(8)	0.5067(11)	0.8208(21)
	6.4527	0.135543	8	0.6133(8)	0.5101(21)	0.8316(35)
	6.6350	0.135340	10	0.6112(11)	0.5078(19)	0.8307(35)
	6.7750	0.135121	12	0.6076(7)	0.5061(14)	0.8329(24)
	7.0203	0.134707	16	0.6063(7)	0.5097(11)	0.8406(21)

Table A.2: Results for the step scaling function Σ_P .

$\bar{g}^2(L)$	β	κ	L/a	$Z_{\Lambda}^{\text{stat}}(g_0, L/a)$	$Z_{\Lambda}^{\text{stat}}(g_0, 2L/a)$	$\Sigma_{\Lambda}^{\text{stat}}(u, a/L)$
1.0989	9.5030	0.131514	6	0.8926(7)	0.8698(8)	0.9745(12)
	9.7500	0.131312	8	0.8860(7)	0.8668(11)	0.9782(14)
	10.0577	0.131079	12	0.8800(6)	0.8630(11)	0.9806(14)
	10.3419	0.130876	16	0.8786(7)	0.8586(16)	0.9773(20)
1.3293	8.6129	0.132380	6	0.8733(8)	0.8458(9)	0.9686(13)
	8.8500	0.132140	8	0.8677(9)	0.8418(13)	0.9701(18)
	9.1859	0.131814	12	0.8635(7)	0.8401(13)	0.9729(17)
	9.4381	0.131589	16	0.8593(9)	0.8361(19)	0.9731(25)
1.4300	8.5598	0.132453	8	0.8593(7)	0.8328(13)	0.9692(17)
	8.9003	0.132095	12	0.8545(7)	0.8314(14)	0.9731(18)
	9.1415	0.131855	16	0.8516(6)	0.8238(23)	0.9674(28)
1.5553	7.9993	0.133118	6	0.8572(6)	0.8246(13)	0.9619(16)
	8.2500	0.132821	8	0.8517(6)	0.8248(13)	0.9684(17)
	8.5985	0.132427	12	0.8459(8)	0.8190(14)	0.9683(20)
	8.8323	0.132169	16	0.8425(9)	0.8141(20)	0.9662(26)
1.6950	7.9741	0.133179	8	0.8414(9)	0.8069(18)	0.9590(24)
	8.3218	0.132756	12	0.8359(8)	0.8074(13)	0.9659(19)
	8.5479	0.132485	16	0.8329(13)	0.8081(19)	0.9703(28)
1.8811	7.4082	0.133961	6	0.8362(7)	0.7939(7)	0.9495(11)
	7.6547	0.133632	8	0.8290(6)	0.7903(17)	0.9533(21)
	7.9993	0.133159	12	0.8247(7)	0.7907(12)	0.9588(16)
	8.2415	0.132847	16	0.8221(13)	0.7898(23)	0.9607(32)
2.1000	7.3632	0.134088	8	0.8193(10)	0.7732(20)	0.9436(26)
	7.6985	0.133599	12	0.8117(9)	0.7756(25)	0.9555(32)
	7.9560	0.133229	16	0.8081(12)	0.7704(21)	0.9533(29)
2.4484	6.7807	0.134994	6	0.8035(8)	0.7420(12)	0.9235(18)
	7.0197	0.134639	8	0.7945(7)	0.7444(19)	0.9370(26)
	7.2025	0.134380	10	0.7936(9)	0.7431(17)	0.9363(24)
	7.3551	0.134141	12	0.7930(10)	0.7465(17)	0.9414(24)
	7.6101	0.133729	16	0.7907(8)	0.7444(16)	0.9415(22)
2.7700	6.5512	0.135327	6	0.7886(9)	0.7133(19)	0.9045(26)
	6.7860	0.135056	8	0.7791(12)	0.7187(24)	0.9225(35)
	6.9720	0.134770	10	0.7786(9)	0.7223(23)	0.9276(31)
	7.1190	0.134513	12	0.7740(11)	0.7220(17)	0.9329(25)
	7.3686	0.134114	16	0.7755(16)	0.7281(30)	0.9388(43)
3.4800	6.2204	0.135470	6	0.7587(10)	0.6562(39)	0.8649(53)
	6.4527	0.135543	8	0.7496(11)	0.6624(29)	0.8837(41)
	6.6350	0.135340	10	0.7477(11)	0.6658(31)	0.8906(43)
	6.7750	0.135121	12	0.7451(11)	0.6696(22)	0.8988(32)
	7.0203	0.134707	16	0.7470(10)	0.6792(24)	0.9092(34)

Table A.3: Results for the step scaling function $\Sigma_{\Lambda}^{\text{stat}}$ (in the ‘new’ scheme).

$\bar{g}^2(L)$	β	κ	L/a	$Z_{A,old}^{stat}(g_0, L/a)$	$Z_{A,old}^{stat}(g_0, 2L/a)$	$\Sigma_{A,old}^{stat}(u, a/L)$
1.0989	9.5030	0.131514	6	0.8903(8)	0.8676(8)	0.9745(12)
	9.7500	0.131312	8	0.8846(7)	0.8635(11)	0.9762(14)
	10.0577	0.131079	12	0.8791(5)	0.8628(14)	0.9814(17)
	10.3419	0.130876	16	0.8773(9)	0.8601(21)	0.9804(26)
1.3293	8.6129	0.132380	6	0.8721(9)	0.8430(10)	0.9666(16)
	8.8500	0.132140	8	0.8664(10)	0.8428(14)	0.9728(19)
	9.1859	0.131814	12	0.8616(6)	0.8351(19)	0.9693(23)
	9.4381	0.131589	16	0.8580(10)	0.8370(48)	0.9755(57)
1.4300	8.5598	0.132453	8	0.8577(8)	0.8325(14)	0.9706(19)
	8.9003	0.132095	12	0.8535(6)	0.8332(21)	0.9761(26)
	9.1415	0.131855	16	0.8488(6)	0.8172(55)	0.9628(65)
1.5553	7.9993	0.133118	6	0.8552(7)	0.8243(19)	0.9639(23)
	8.2500	0.132821	8	0.8497(6)	0.8224(17)	0.9678(22)
	8.5985	0.132427	12	0.8441(8)	0.8198(26)	0.9712(32)
	8.8323	0.132169	16	0.8410(12)	0.8203(57)	0.9754(69)
1.6950	7.9741	0.133179	8	0.8411(11)	0.8079(20)	0.9606(26)
	8.3218	0.132756	12	0.8340(8)	0.8154(32)	0.9777(39)
	8.5479	0.132485	16	0.8328(16)	0.8076(87)	0.970(11)
1.8811	7.4082	0.133961	6	0.8336(7)	0.7904(7)	0.9482(12)
	7.6547	0.133632	8	0.8269(7)	0.7921(21)	0.9578(27)
	7.9993	0.133159	12	0.8232(5)	0.7863(20)	0.9551(25)
	8.2415	0.132847	16	0.8210(18)	0.798(12)	0.972(15)
2.1000	7.3632	0.134088	8	0.8172(13)	0.7778(24)	0.9518(33)
	7.6985	0.133599	12	0.8097(8)	0.7757(67)	0.9579(83)
	7.9560	0.133229	16	0.8091(21)	0.786(12)	0.971(14)
2.4484	6.7807	0.134994	6	0.8016(9)	0.7416(17)	0.9252(23)
	7.0197	0.134639	8	0.7941(9)	0.7399(37)	0.9317(48)
	7.2025	0.134380	10	0.7932(9)	0.7422(37)	0.9357(48)
	7.3551	0.134141	12	0.7901(13)	0.7382(54)	0.9344(70)
	7.6101	0.133729	16	0.7870(9)	0.756(13)	0.961(17)
2.7700	6.5512	0.135327	6	0.7863(10)	0.7132(34)	0.9070(45)
	6.7860	0.135056	8	0.7804(15)	0.7169(45)	0.9185(60)
	6.9720	0.134770	10	0.7759(10)	0.7121(55)	0.9177(72)
	7.1190	0.134513	12	0.7739(12)	0.7152(72)	0.9241(95)
	7.3686	0.134114	16	0.7732(30)	0.681(34)	0.880(43)
3.4800	6.2204	0.135470	6	0.7573(9)	0.6558(24)	0.8659(34)
	6.4527	0.135543	8	0.7501(9)	0.6560(77)	0.874(10)
	6.6350	0.135340	10	0.7476(15)	0.661(11)	0.885(15)
	6.7750	0.135121	12	0.7430(10)	0.659(16)	0.886(21)
	7.0203	0.134707	16	0.7474(13)	0.642(46)	0.859(61)

Table A.4: Results for the step scaling function $\Sigma_{A,old}^{stat}$ (in the ‘old’ scheme).

A.3 Continuum extrapolation of Σ_A^{stat}

For fixed coupling u the step scaling function defined in Eq. (A.20) has a continuum limit, $\sigma_A^{\text{stat}}(u)$. Neglecting for the moment the uncertainties on the correct values of c_t , \tilde{c}_t and c_A^{stat} , we expect the leading-order cutoff effects to be quadratic in the lattice spacing,

$$\Sigma_A^{\text{stat}}(u, a/L) = \sigma_A^{\text{stat}}(u) + \mathcal{O}(a^2/L^2), \quad (\text{A.23})$$

since $\mathcal{O}(a)$ improvement is employed. Based on this ansatz, Figure 5 in Section 3 illustrates the continuum extrapolation of Σ_A^{stat} for a representative subset of our available coupling values $u = \bar{g}^2(L)$. The coarsest lattices (with $L/a = 6$) have been omitted from the fits as a safeguard against higher order cutoff effects. For the remaining $a/L \leq 1/8$, the one-loop cutoff effects are quite small, see Figure B.2.

Although these extrapolations are entirely compatible with an approach to the continuum limit quadratic in a/L , we also have investigated extrapolations linear in a/L . These as well yield reasonable fits with consistent results and even comparable total χ^2/dof (when summing up the χ^2 -s belonging to the individual fits at the ten u -values) so that the form of the lattice spacing dependence can not be decided on the basis of the data. Therefore, we have studied the influence of the imperfect (i.e. only perturbative) knowledge of some of the improvement coefficients in more detail.

Since the usage of the two-loop approximation (A.21) for c_t in the calculation of the correlation functions (and thereby also in the step scaling function Σ_A^{stat}) should cancel the main contributions from the related boundary terms, we only address its effect originating from the fixing of the renormalized coupling, the values of which were taken over from Ref. [13] with c_t still set to one-loop. Changing c_t from one- to two-loop also in this step then requires to adjust the bare coupling and the value of the critical quark mass accordingly before the simulations for Σ_A^{stat} can be performed. We have done this analysis for the largest fixed coupling, $u = 3.48$, where the uncertainty in c_t is largest and thus its effect most pronounced. At $L/a = 6$ the resulting change in Σ_A^{stat} turns out to lie clearly inside the statistical errors, and this effect will even get smaller for decreasing a/L . On the other hand, if we just compute Σ_A^{stat} with the one-loop value of c_t as in the computation of the coupling, we found the results, now for $u = 2.77$ and $L/a = 6, 8$, to be indistinguishable within errors, too. We conclude that any small uncertainty present in c_t beyond the available two-loop estimate is numerically unimportant for the cutoff dependence of Σ_A^{stat} .

Regarding the $\mathcal{O}(a)$ improvement coefficient \tilde{c}_t , we followed the same line as in [13] and assessed its influence on our results by artificially replacing the one-loop coefficient in the expression (A.22) by ten times its value. I.e. we set \tilde{c}_t to $\tilde{c}_t' = 1 - 0.180 g_0^2$ in some additional simulations at $u = 3.48$, and the outcome is that the corresponding estimates on Σ_A^{stat} for $L/a = 6$ still differ by around 1.5%, while for $L/a = 8$ they already agree within their statistical errors. As this difference drops further for growing L/a and/or smaller couplings, a possible imperfection of \tilde{c}_t does not affect the results on Σ_A^{stat} either.

Finally, we also checked for the influence of the $\mathcal{O}(a)$ improvement coefficient in the static-light axial current, c_A^{stat} , by analyzing our data with $c_A^{\text{stat}} = 0$ instead of the one-loop value (A.9). Whereas the related change in Z_A^{stat} is of the order of a few percent and hence still substantial, it largely cancels in the ratio of Eq. (A.20) so that this effect is no more significant for Σ_A^{stat} given its statistical errors.

All in all these findings demonstrate that at the level of our precision linear a -effects

in the data on Σ_A^{stat} are negligible, and extrapolations using $(a/L)^2$ -terms as the dominant scaling violation are justified indeed.

Appendix B Perturbation theory

This appendix provides a few details on the perturbative computations, which were required to obtain the one-loop expression for $h(d/L, u)$, Eq. (2.12), the two-loop anomalous dimension and the one-loop estimates of the discretization errors of the step scaling function Σ_A^{stat} . Note that here we restrict ourselves to the case of the modified (or ‘new’) scheme introduced via Eq. (2.15) in this paper, because the perturbation theory of the original scheme defined through Eq. (2.7) has been extensively discussed already in Ref. [17] where also more details on the different steps involved can be found.

The correlation functions f_A^{stat} , $f_{\delta A}^{\text{stat}}$ and f_1 are expanded in powers of the coupling g_0^2 as explained in [17] and [62], and the analogous expansion of f_1^{hh} is explained below.

B.1 The correlation function f_1^{hh}

After integrating out the static quark fields, the correlation function f_1^{hh} can be written as

$$f_1^{\text{hh}}(x_3) = \frac{a^2}{L^2} \sum_{x_1, x_2} \left\langle \text{tr} \left\{ U(x, 0) U(x + a\hat{0}, 0) \cdots U(x + (L - a)\hat{0}, 0) \right. \right. \\ \left. \left. \times U((L - a)\hat{0}, 0)^{-1} U((L - 2a)\hat{0}, 0)^{-1} \cdots U(0, 0)^{-1} \right\} \Big|_{x_0=0} \right\rangle, \quad (\text{B.1})$$

where the trace is taken over colour indices only.

Writing $U(x, \mu) = \exp \{g_0 a q_\mu(x)\}$, with the gluon field $q_\mu(x) = q_\mu^a(x) T^a$, where T^a are the antihermitian generators of the gauge group, the function f_1^{hh} can be expanded in the bare coupling,

$$f_1^{\text{hh}}(d) = 3 + g_0^2 f_1^{\text{hh},(1)}(d) + \mathcal{O}(g_0^4), \quad d = |x_3|. \quad (\text{B.2})$$

Determining the one-loop coefficient $f_1^{\text{hh},(1)}$ amounts to calculating and summing the diagrams shown in Figure B.1 using the gluon propagator $D_{\mu\nu}(x, y)$ (with SF boundary conditions) given in Ref. [58].

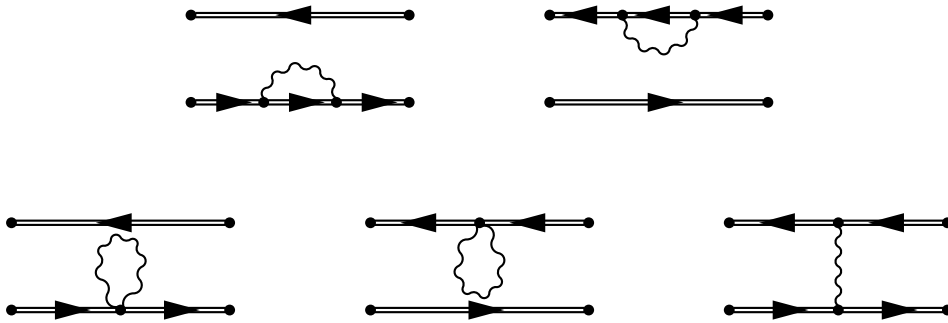


Figure B.1: One-loop diagrams contributing to f_1^{hh} . The two dots on the left are at $x_0 = 0$, the dots on the right are at $x_0 = L$.

For comparison with the non-perturbative results shown in Figure 4, Subsection 2.2, we consider the one-loop coefficient $h^{(1)}(d/L)$ of Eq. (2.13), which reads

$$h^{(1)}(d/L) = \frac{1}{3} \left\{ f_1^{\text{hh},(1)}(d) - f_1^{\text{hh},(1)}(L/2) \right\}, \quad (\text{B.3})$$

and which we can obtain analytically. (For the other quantities considered in this appendix, the diagrams are calculated numerically.) Only the last of the diagrams in Figure B.1 contributes, and we thus can write

$$\begin{aligned} h^{(1)}(d/L) &= \frac{4a^6}{3L^4} \sum_{x_0, y_0} \sum_{x_1, y_1} \sum_{x_2, y_2} \{ D_{00}(x, y)|_{x_3=d, y_3=0} - D_{00}(x, y)|_{x_3=L/2, y_3=0} \} \\ &= \frac{4a^2}{3L^3} \sum_{p_3} \left\{ e^{ip_3 d} - e^{ip_3 L/2} \right\} \sum_{x_0, y_0} d_{00}(x_0, y_0; (0, 0, p_3)), \end{aligned} \quad (\text{B.4})$$

with the momentum-space gluon propagator $d_{00}(x_0, y_0; \mathbf{p})$ defined in Ref. [58]. The $p_3 = 0$ term does not contribute to the sum, and using the explicit form of $d_{00}(x_0, y_0; \mathbf{p})$ for $\mathbf{p} \neq \mathbf{0}$, one can show that

$$a^2 \sum_{x_0, y_0} d_{00}(x_0, y_0; (0, 0, p_3)) = \frac{L}{\hat{p}_3^2} \quad (\text{B.5})$$

with $\hat{p}_3 = \frac{2}{a} \sin\left(\frac{ap_3}{2}\right)$. Thus we see that $h^{(1)}(d/L)$ is just given in terms of the one-dimensional scalar propagator on a periodic lattice with length L , which has *no lattice artifacts*. This eventually leads to the result quoted in Eq. (2.14). The absence of any lattice spacing dependence is a consequence of the special kinematics, namely the summation over x_1, x_2 , but will of course not be exact in higher orders of perturbation theory.

B.2 Anomalous dimensions

In order to precisely connect to the RGI current, it is important to obtain the anomalous dimension of the static-light axial current in the SF scheme at two-loop order. The anomalous dimension is expanded as

$$\gamma(\bar{g}) = -\bar{g}^2 \left\{ \gamma_0 + \gamma_1^{\text{SF}} \bar{g}^2 + \text{O}(\bar{g}^4) \right\}, \quad (\text{B.6})$$

with $\gamma_0 = -1/(4\pi^2)$ and the two-loop anomalous dimension in the SF scheme, γ_1^{SF} .

With the perturbative expansions for the various correlation functions, the ratio Ξ_{I} of Eq. (A.16) can be written as a series

$$\Xi_{\text{I}}(g_0, a/L) = \Xi_{\text{I}}^{(0)}(a/L) + g_0^2 \Xi_{\text{I}}^{(1)}(a/L) + \text{O}(g_0^4). \quad (\text{B.7})$$

Accordingly, this allows us to expand the SF renormalization constant $Z_{\text{A}}^{\text{stat}} = \Xi_{\text{I}}^{(0)}/\Xi_{\text{I}}$ (see Eq. (A.19)) as

$$Z_{\text{A}}^{\text{stat}} = Z_{\text{A}}^{\text{stat},(0)} + g_0^2 Z_{\text{A}}^{\text{stat},(1)} + \text{O}(g_0^4). \quad (\text{B.8})$$

With the one-loop relation between the bare lattice current and the renormalized static axial current in the $\overline{\text{MS}}$ scheme, the anomalous dimension in the $\overline{\text{MS}}$ scheme, Eq. (5.5) [38, 39, 40], can be converted into the SF scheme. The renormalization constant relating the SF scheme and the $\overline{\text{MS}}$ scheme is obtained from the relation between the SF scheme and the

bare lattice current, Eq. (B.8), the connection of the bare lattice current and a ‘matching scheme’ [63, 64] and the relation between the latter and the $\overline{\text{MS}}$ scheme [30]. Here the matching scheme is defined by the requirement that the renormalized static-light axial current at scale $\mu = m_h$ equals the relativistic axial current with a heavy quark mass m_h up to terms of $\mathcal{O}(1/m_h)$, and the current in the relativistic theory is normalized by current algebra (imposing the chiral Ward identities).⁶ Following the steps in Ref. [17], this analysis finally yields

$$\theta = 0.0 : \quad \gamma_1^{\text{SF}} = \frac{1}{(4\pi)^2} \{ 0.22(2) - 0.0552(13)N_f \}, \quad (\text{B.9})$$

$$\theta = 0.5 : \quad \gamma_1^{\text{SF}} = \frac{1}{(4\pi)^2} \{ 0.10(2) - 0.0477(13)N_f \}, \quad (\text{B.10})$$

$$\theta = 1.0 : \quad \gamma_1^{\text{SF}} = \frac{1}{(4\pi)^2} \{ -0.08(2) - 0.0365(13)N_f \}. \quad (\text{B.11})$$

B.3 Discretization errors

The one-loop expansion at hand is also helpful to study discretization errors in the step scaling function. Using Eq. (B.8), the step scaling function at lattice spacing a is expanded as

$$\Sigma_A^{\text{stat}}(u, a/L) = 1 + u \Sigma_A^{\text{stat},(1)}(a/L) + \mathcal{O}(u^2), \quad (\text{B.12})$$

and its continuum limit $\sigma_A^{\text{stat}}(u)$ as

$$\sigma_A^{\text{stat}}(u) = 1 + u \sigma_A^{\text{stat},(1)} + u^2 \sigma_A^{\text{stat},(2)} + \mathcal{O}(u^3), \quad (\text{B.13})$$

with

$$\begin{aligned} \sigma_A^{\text{stat},(1)} &= \ln(2) \gamma_0, \\ \sigma_A^{\text{stat},(2)} &= \frac{1}{2} \ln^2(2) \gamma_0^2 + \ln^2(2) b_0 \gamma_0 + \ln(2) \gamma_1. \end{aligned} \quad (\text{B.14})$$

As a measure for the discretization errors, we define

$$\delta(u, a/L) = \frac{\Sigma_A^{\text{stat}}(u, a/L) - \sigma_A^{\text{stat}}(u)}{\sigma_A^{\text{stat}}(u)} \quad (\text{B.15})$$

with a perturbative expansion

$$\delta(u, a/L) = \delta^{(1)}(a/L) u + \mathcal{O}(u^2). \quad (\text{B.16})$$

The one-loop coefficient $\delta^{(1)}$ versus the lattice spacing squared is shown in Figure B.2 for different values of θ . In the range of lattice spacings where our non-perturbative calculation is performed, the discretization errors at one-loop level are smaller than $1\% \times u$, giving rise to the hope that also the non-perturbative discretization errors are reasonably small. A welcome feature of $\delta^{(1)}$ at $\theta = 0.5$ is that it is entirely dominated by the leading a^2/L^2 -term in the a -expansion.

⁶Since the wording in Ref. [17] is not completely clear on this, we point out that $A_{\overline{\text{MS}}}^{\text{stat}}$ in that reference refers to what we call the $\overline{\text{MS}}$ scheme here as well as in Ref. [17].

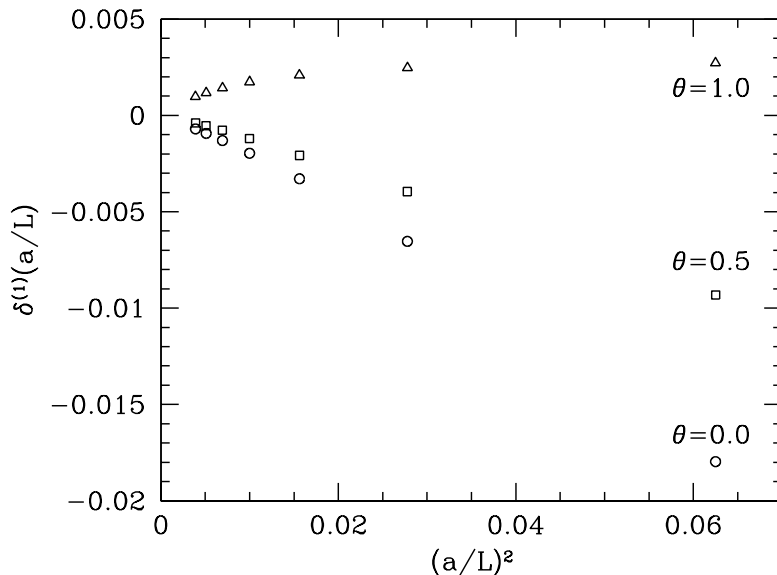


Figure B.2: Discretization errors of the step scaling function at one-loop level. The continuum extrapolation of the non-perturbative results uses $(a/L)^2 < 0.02$.

Appendix C Continuum step scaling function and matching at $L = 1.436 r_0$

In this last appendix we briefly discuss our parametrization (i.e. the interpolating fit) of the continuum step scaling function and some details on the calculation of Z_A^{stat} at the matching scale $2L_{\text{max}} = 1.436 r_0$.

C.1 Fits and error determination in the scale evolution

As described in Appendix A.3, the continuum step scaling function $\sigma_A^{\text{stat}}(u)$ has been obtained by extrapolating the lattice data on $\Sigma_A^{\text{stat}}(u, a/L)$ at fixed u to the continuum limit. The next step is now to solve the recursion specified through Eqs. (3.1) – (3.4). In practice this is done by first representing the results for $\sigma_A^{\text{stat}}(u)$ in Table 1 by a fit and then solving the recursion, Eq. (3.4), with $\sigma_A^{\text{stat}}(u)$ given by the fit function.

Guided by the analysis for the step scaling function of the pseudoscalar density σ_P in Ref. [13] and the perturbative expansion discussed in Appendix B.3,

$$\sigma_A^{\text{stat}}(u) = 1 + s_0 u + s_1 u^2 + s_2 u^3 + \dots + s_n u^{n+1} \quad (\text{C.1})$$

is chosen as fit ansatz. The two non-trivial leading terms are restricted by perturbation theory,

$$s_0 = \sigma_A^{\text{stat},(1)}, \quad s_1 = \sigma_A^{\text{stat},(2)}, \quad (\text{C.2})$$

cf. Eqs. (B.14). Up to three additional free fit parameters were allowed for. All of these fits represent the data in Table 1 well, and we decided to quote the two-parameter fit (the curve of which is shown in Figure 6) as the final result for the functional form of σ_A^{stat} . To check that the polynomial fits are stable, we also investigated fits where only s_0 or even no

coefficient at all is constrained to its perturbative value. This leads to consistent results for $\sigma_{\text{A}}^{\text{stat}}(u)$; particularly the latter fit then reproduces the perturbative prediction for s_0 .

Having chosen a definite expression for $\sigma_{\text{A}}^{\text{stat}}(u)$, the solution of the associated recursion is unique. Since the errors on the step scaling function stem from different simulation runs and are hence uncorrelated, the errors on the fit parameters in the polynomial (C.1) for $\sigma_{\text{A}}^{\text{stat}}(u)$ and those on the v_k -s calculated from it can be estimated straightforwardly by the standard error propagation rules. Finally, by increasing the number of free fit parameters (while fixing s_0, s_1 to perturbation theory) as mentioned above, we convinced ourselves that the systematic error induced by the choice of fit functions is well under control: in fact, we then observed the expected pattern of finding slightly different errors but compatible results at comparably good overall fit quality.

C.2 Calculation of $Z_{\text{A}}^{\text{stat}}$ at the low-energy matching scale

The total renormalization factor Z_{RGI} introduced in Section 4 involves the value of the renormalization constant $Z_{\text{A}}^{\text{stat}}$ at our particular matching point: $Z_{\text{A}}^{\text{stat}}(g_0, L/a)|_{L=1.436 r_0}$. As the latter connects a bare matrix element of the static-light axial current to the one renormalized in the SF scheme, this amounts to calculate $Z_{\text{A}}^{\text{stat}}$ for a range of bare couplings commonly used in simulations in physically large volumes.

To extract $Z_{\text{A}}^{\text{stat}}$ we exploit the fact that the required pairs $(L/a, \beta)$ that match the condition $L/a = 1.436 r_0/a$ have already been determined for the relevant β -range in Appendix C of [13] by utilizing the known parametrization of $\ln(a/r_0)$ in terms of β from Ref. [34]. We thus could take over these pairs and computed $Z_{\text{A}}^{\text{stat}}$ for $\theta = 0.5$ from the renormalization condition (A.19) at the corresponding values $\kappa = \kappa_c$ of the critical hopping parameter [65]. The results for $Z_{\text{A}}^{\text{stat}}(g_0, L/a)|_{L=1.436 r_0}$ using the one- and two-loop expressions for c_t , cf. Eq. (A.21), are given in Table C.1. The difference originating from the two

L/a	$\beta = 6/g_0^2$	$c_t^{2\text{-loop}}$		$c_t^{1\text{-loop}}$	
		κ	$Z_{\text{A}}^{\text{stat}}$	κ	$Z_{\text{A}}^{\text{stat}}$
8	6.0219	0.13508	0.6926(15)	0.13504	0.6932(10)
10	6.1628	0.13565	0.6810(17)	0.13564	0.6824(16)
12	6.2885	0.13575	0.6786(18)	0.13574	0.6795(16)
16	6.4956	0.13559	0.6777(17)	0.13558	0.6763(18)

Table C.1: Results for $Z_{\text{A}}^{\text{stat}}(g_0, L/a)$ at fixed scale $L = 2L_{\text{max}} = 1.436 r_0$ with c_t being set to either one- or two-loop. The critical κ -values $\kappa = \kappa_c$ [65] are the same as used for Table C.1 of Ref. [13].

perturbative approximations for c_t is completely covered by the statistical errors so that we again consider $c_t^{2\text{-loop}}$ to already account for the dominant part of the boundary cutoff effects in the gauge sector. Similarly to the discussion in Appendix A.3, the influence of the boundary improvement coefficient \tilde{c}_t in the fermionic sector can also be neglected at the level of our precision. The parametrization of the results for $Z_{\text{A}}^{\text{stat}}(g_0, L/a)|_{L=1.436 r_0}$ by a polynomial fit in $(\beta - 6)$, with $c_t^{2\text{-loop}}$ and $c_{\text{A}}^{\text{stat}}$ from one-loop perturbation theory, is quoted in Section 4, where the coefficients in the first block of Table 2 are to be combined with Eq. (4.1). The

smooth dependence of Z_A^{stat} on β in the studied region of bare couplings suggests that this representation can also be slightly extended down to $\beta = 6.0$ (even though we could not directly simulate that point for the same reason as in case of Z_P [13]), and we therefore regard it as a reliable representation of our data over the whole range $6.0 \leq \beta \leq 6.5$.

As in Appendix A.3, we also set $c_A^{\text{stat}} = 0$ instead of one-loop in the analysis of the data on $Z_A^{\text{stat}}(g_0, L/a)|_{L=1.436 r_0}$, and the results are listed in the middle part of Table C.2. In contrast

L/a	$\beta = 6/g_0^2$	$c_A^{\text{stat}} = 0$		$c_{\text{sw}} = 0$	
		κ	Z_A^{stat}	κ	Z_A^{stat}
4	5.6791	—	—	0.15268	0.6923(13)
6	5.8636	—	—	0.15451	0.6315(16)
8	6.0219	0.13508	0.6736(14)	0.15341	0.6075(13)
10	6.1628	0.13565	0.6633(17)	0.15202	0.5964(18)
12	6.2885	0.13575	0.6621(17)	0.15078	0.5971(32)
16	6.4956	0.13559	0.6627(17)	0.14887	0.5991(52)

Table C.2: Results for $Z_A^{\text{stat}}(g_0, L/a)$ at fixed scale $L = 2L_{\text{max}} = 1.436 r_0$ for $c_A^{\text{stat}} = 0$ and unimproved Wilson fermions (i.e. $c_{\text{sw}} = 0$ and thus, $c_A = c_A^{\text{stat}} = 0$ too), where c_t was kept at its two-loop value.

to the step scaling function, which did not change appreciably under this replacement of the value for c_A^{stat} , we observe an effect of about 3% in Z_A^{stat} at the low-energy matching scale $L = 2L_{\text{max}} = 1.436 r_0$.

Furthermore, we addressed the case of unimproved Wilson fermions by also setting $c_{\text{sw}} = 0$ in the relativistic fermion action and, after having computed the needed estimates of the critical hopping parameter for this situation, carried out the additional runs to determine the renormalization constant. In this case the pairs $(L/a, \beta)$ were extended to lower values of β in order to be able to make contact with the β -region that is typically employed in simulations to calculate the bare matrix element defining the B-meson decay constant, as e.g. those in Refs. [10, 11]. The resulting estimates on Z_A^{stat} are shown in the right part of Table C.2, and the corresponding polynomial representations for both aforementioned cases are as well found via Eq. (4.1) together with the two lower blocks of Table 2.

We conclude this discussion with the general remark that the uncertainties of the entering critical κ -values (of 1–2 and 2–4 on the last decimal place in the case of $c_{\text{sw}} =$ non-perturbative and $c_{\text{sw}} = 0$, respectively) do not affect the Z -factors significantly.

References

- [1] N. Yamada, Nucl. Phys. Proc. Suppl. 119 (2003) 93, hep-lat/0210035.
- [2] M. Guagnelli et al., Phys. Lett. B546 (2002) 237, hep-lat/0206023.
- [3] M. Guagnelli et al., Nucl. Phys. Proc. Suppl. 119 (2003) 616, hep-lat/0209113.
- [4] E. Eichten and B. Hill, Phys. Lett. B234 (1990) 511.

- [5] C.R. Allton et al., Nucl. Phys. B349 (1991) 598.
- [6] C. Alexandrou et al., Phys. Lett. B256 (1991) 60.
- [7] APE, C.R. Allton et al., Phys. Lett. B326 (1994) 295, hep-ph/9402343.
- [8] C. Alexandrou et al., Nucl. Phys. B414 (1994) 815, hep-lat/9211042.
- [9] C.W. Bernard, J.N. Labrenz and A. Soni, Phys. Rev. D49 (1994) 2536, hep-lat/9306009.
- [10] A. Duncan et al., Phys. Rev. D51 (1995) 5101, hep-lat/9407025.
- [11] T. Draper and C. McNeile, Nucl. Phys. Proc. Suppl. 34 (1994) 453, hep-lat/9401013.
- [12] UKQCD, A.K. Ewing et al., Phys. Rev. D54 (1996) 3526, hep-lat/9508030.
- [13] ALPHA, S. Capitani et al., Nucl. Phys B544 (1999) 669, hep-lat/9810063.
- [14] R. Sommer, Nucl. Phys. Proc. Suppl. 119 (2003) 185, hep-lat/0209162.
- [15] J. Heitger, Applications of Non-perturbative Renormalization, Contribution to 30th International Conference on High-Energy Physics (ICHEP 2000), Osaka, Japan, 27 July – 2 August 2000, hep-ph/0010050.
- [16] ALPHA, J. Heitger, M. Kurth and R. Sommer, Nucl. Phys. Proc. Suppl. 119 (2003) 607, hep-lat/0209078.
- [17] ALPHA, M. Kurth and R. Sommer, Nucl. Phys. B597 (2001) 488, hep-lat/0007002.
- [18] M. Lüscher et al., Nucl. Phys. B384 (1992) 168, hep-lat/9207009.
- [19] S. Sint, Nucl. Phys. B421 (1994) 135, hep-lat/9312079.
- [20] S. Sint and R. Sommer, Nucl. Phys. B465 (1996) 71, hep-lat/9508012.
- [21] ALPHA, M. Lüscher et al., Nucl. Phys. B478 (1996) 365, hep-lat/9605038.
- [22] M. Lüscher, P. Weisz and U. Wolff, Nucl. Phys. B359 (1991) 221.
- [23] M. Lüscher et al., Nucl. Phys. B389 (1993) 247, hep-lat/9207010.
- [24] M. Lüscher et al., Nucl. Phys. B413 (1994) 481, hep-lat/9309005.
- [25] R. Sommer, Non-perturbative Renormalization of QCD, Lectures given at 36th Internationale Universitätswochen für Kernphysik und Teilchenphysik, Schladming, Austria, 1 – 8 March 1997, hep-ph/9711243.
- [26] M. Lüscher, Advanced Lattice QCD, Lectures given at Les Houches Summer School in Theoretical Physics, Probing the Standard Model of Particle Interactions, Les Houches, France, 28 July – 5 September 1997, hep-ph/9802029.
- [27] ALPHA, S. Sint and P. Weisz, Nucl. Phys B545 (1999) 529, hep-lat/9808013.
- [28] M.A. Shifman and M.B. Voloshin, Sov. J. Nucl. Phys. 45 (1987) 292.

- [29] H.D. Politzer and M.B. Wise, Phys. Lett. B206 (1988) 681.
- [30] E. Eichten and B. Hill, Phys. Lett. B240 (1990) 193.
- [31] G. Parisi, R. Petronzio and F. Rapuano, Phys. Lett. B128 (1983) 418.
- [32] K. Symanzik, Nucl. Phys. B226 (1983) 187.
- [33] R. Sommer, Nucl. Phys. B411 (1994) 839, hep-lat/9310022.
- [34] ALPHA, M. Guagnelli, R. Sommer and H. Wittig, Nucl. Phys. B535 (1998) 389, hep-lat/9806005.
- [35] ALPHA, M. Lüscher et al., Nucl. Phys. B491 (1997) 323, hep-lat/9609035.
- [36] M. Neubert, Phys. Rept. 245 (1994) 259, hep-ph/9306320.
- [37] M. Beneke, Phys. Rept. 317 (1999) 1, hep-ph/9807443.
- [38] X. Ji and M.J. Musolf, Phys. Lett. B257 (1991) 409.
- [39] D.J. Broadhurst and A.G. Grozin, Phys. Lett. B267 (1991) 105, hep-ph/9908362.
- [40] V. Gimenez, Nucl. Phys. B375 (1992) 582.
- [41] T. van Ritbergen, J.A.M. Vermaseren and S.A. Larin, Phys. Lett. B400 (1997) 379, hep-ph/9701390.
- [42] K.G. Chetyrkin, Phys. Lett. B404 (1997) 161, hep-ph/9703278.
- [43] J.A.M. Vermaseren, S.A. Larin and T. van Ritbergen, Phys. Lett. B405 (1997) 327, hep-ph/9703284.
- [44] ALPHA & UKQCD, J. Garden et al., Nucl. Phys. B571 (2000) 237, hep-lat/9906013.
- [45] ALPHA, M. Guagnelli et al., Nucl. Phys. B595 (2001) 44, hep-lat/0009021.
- [46] H. Leutwyler, Principles of Chiral Perturbation Theory, Lectures given at Hadrons 94 Workshop, Gramado, Brazil, 10 – 14 April 1994, hep-ph/9406283.
- [47] ALPHA, J. Heitger and R. Sommer, Nucl. Phys. Proc. Suppl. 106 (2002) 358, hep-lat/0110016.
- [48] G.P. Lepage and P.B. Mackenzie, Phys. Rev. D48 (1993) 2250, hep-lat/9209022.
- [49] S. Hashimoto, T. Ishikawa and T. Onogi, Nucl. Phys. Proc. Suppl. 106 (2002) 352.
- [50] C. Alexandrou et al., Z. Phys. C62 (1994) 659, hep-lat/9312051.
- [51] R. Sommer, Phys. Rept. 275 (1996) 1, hep-lat/9401037.
- [52] H. Wittig, Heavy Quarks on the Lattice: Status and Perspectives, Lectures given at International School of Physics *Enrico Fermi*, Varenna, Italy, 8 – 18 July 1997, hep-lat/9710088.

- [53] ALPHA, J. Rolf and S. Sint, JHEP 12 (2002) 007, hep-ph/0209255.
- [54] ALPHA, A. Jüttner and J. Rolf, Phys. Lett. B560 (2003) 59, hep-lat/0302016.
- [55] C. Morningstar and J. Shigemitsu, Phys. Rev. D57 (1998) 6741, hep-lat/9712016.
- [56] K.I. Ishikawa, T. Onogi and N. Yamada, Nucl. Phys. Proc. Suppl. 83-84 (2000) 301, hep-lat/9909159.
- [57] ALPHA, A. Bode, P. Weisz and U. Wolff, Nucl. Phys. B576 (2000) 517, hep-lat/9911018.
- [58] M. Lüscher and P. Weisz, Nucl. Phys. B479 (1996) 429, hep-lat/9606016.
- [59] B. Gehrman, Ph.D. Thesis (2002), hep-lat/0207016.
- [60] ALPHA, M. Guagnelli and J. Heitger, Comput. Phys. Commun. 130 (2000) 12, hep-lat/9910024.
- [61] S. Fischer et al., Comput. Phys. Commun. 98 (1996) 20, hep-lat/9602019.
- [62] ALPHA, S. Sint and P. Weisz, Nucl. Phys. B502 (1997) 251, hep-lat/9704001.
- [63] ALPHA, M. Kurth and R. Sommer, Nucl. Phys. B623 (2002) 271, hep-lat/0108018.
- [64] A. Borrelli and C. Pittori, Nucl. Phys. B385 (1992) 502.
- [65] H. Wittig, private communication.